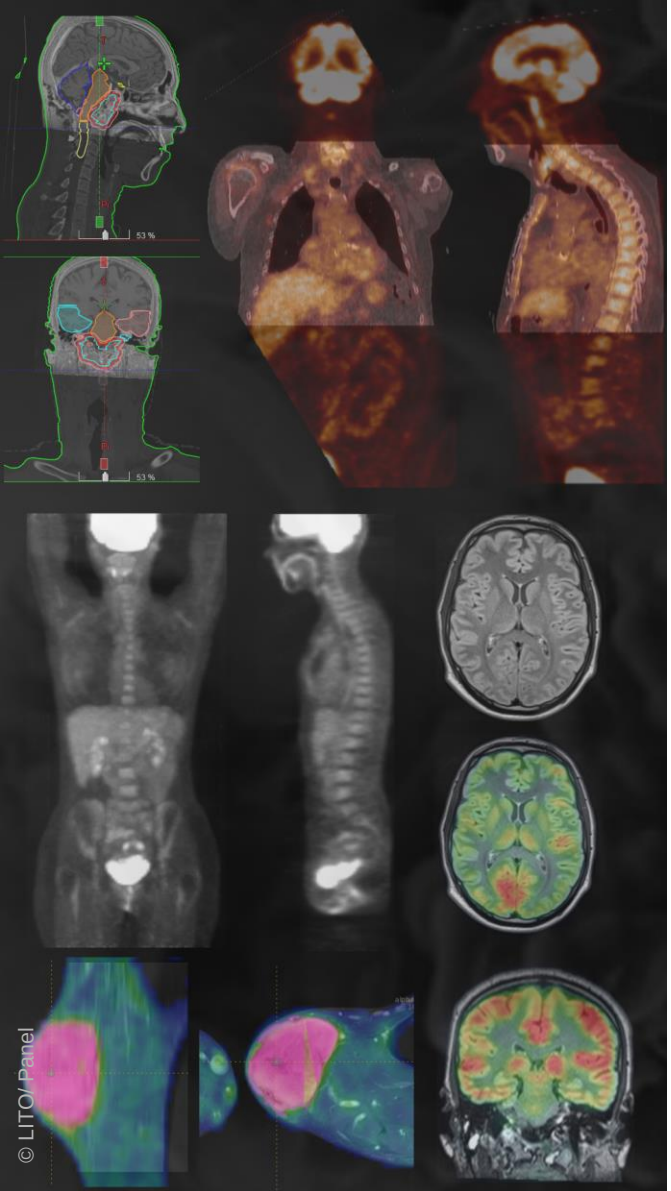

Retour EANM 2021

15/12/2021

Total submitted abstracts: 1272

1088 acceptés (86%, 51% en oral)

Orals Scientific:
395 for a Top Rated Oral Presentation
176 for a Featured Session
26 for Top Trials Session
26 for Case Report Session

Orals Techs:
30 for a top Rated Oral Presentation

e-Poster with Oral Presentation:
Scientific: 241 for an e-Poster
Technologists: 16

e-Poster (only)
Scientific: 170
Technologists: 8

Submissions from 59 countries:

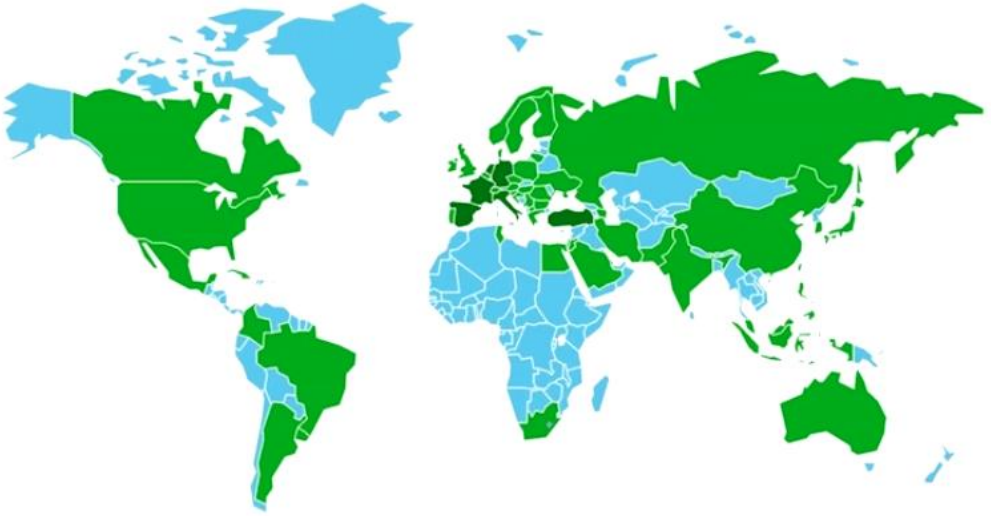

EANM 21 WORLD LEADING MEETING VIRTUAL

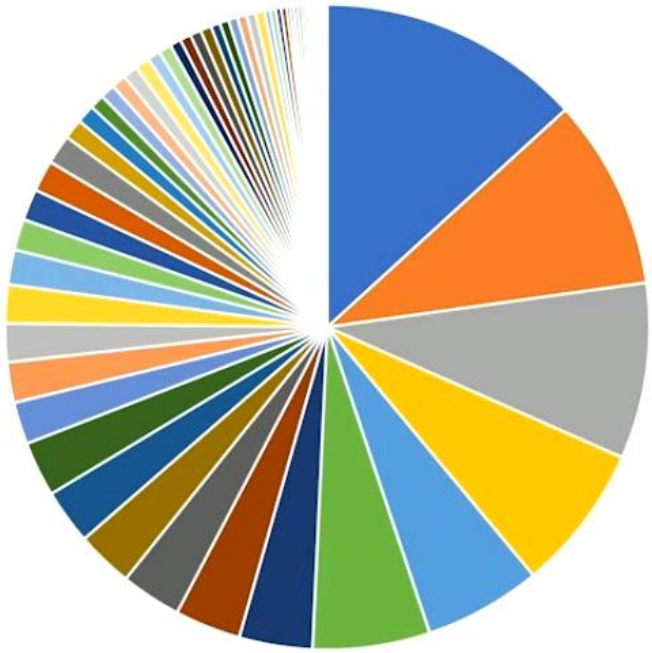

Accepted abstracts:		for HL
	1088	**313**
1. Italy	13.2%	14%
2. Spain	9.6%	
3. Germany	8.8%	
4. France	7.3%	
5. Netherlands	5.9%	
6. Turkey	5.9%	

Abstracts for:	
FDG	123
PSMA	89
FAPI	20
Covid 19	17
Neural Network (AI)	10


PD. Dr. Burger
Prof. Dr. Albert


PD. Dr. Burger
Prof.


PD. Dr. Burger
Prof. Dr. Albert


PD. Dr. Burger
Prof.


PD. Dr. Burger


NUKFLIX
proudly presents...

	ACCREDITED PET/CT CENTRE •2021• RESEARCH4LIFE an EANM initiative OF EXCELLENCE		
			

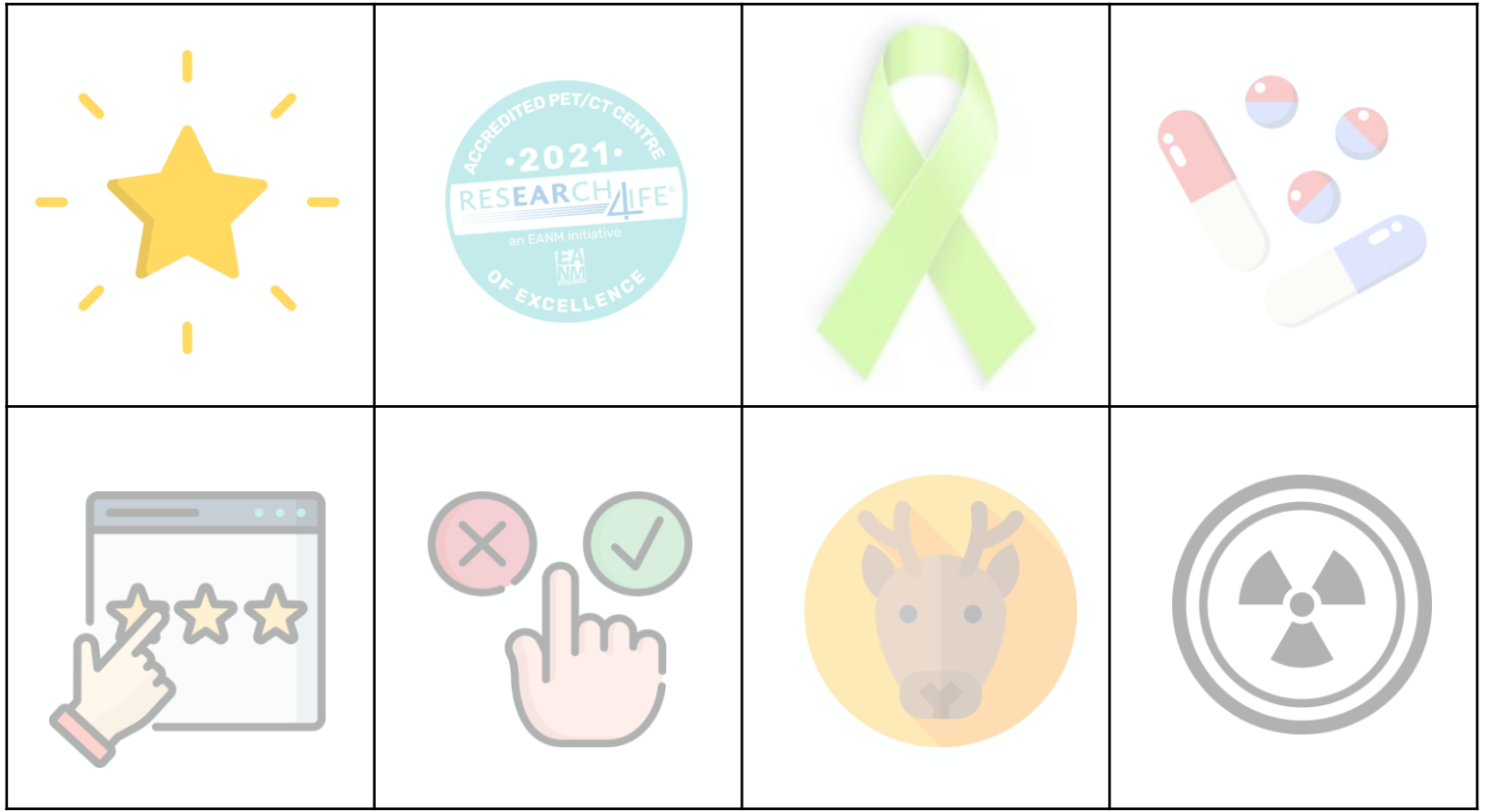
ACCREDITED PET/CT CENTRE
•2021•
RESEARCH4LIFE
an EANM initiative
OF EXCELLENCE

FACULTY OF MEDICINE AND HEALTH SCIENCES

DEPARTMENT OF HEAD AND SKIN
RESEARCH GROUP HEAD AND NECK SURGERY

DO WE KNOW WHAT WE'RE LOOKING AT?

INCREASING OUR UNDERSTANDING OF ^{18}F-FDG DISTRIBUTION IN ONCOLOGY BY DIRECT COREGISTRATION OF HISTOPATHOLOGY AND AUTORADIOGRAPHY IN MALIGNANCIES OF THE HEAD AND NECK

Jens Debacker, David Creytens, Yves D'Asseler, Kathia De Man, Benedicte Descamps, Vincent Keereman, Sasha Libbrecht, Vanessa Schelfhout, Koen Van de Vijver, Christian Vanhove and Wouter Huvenne

GHENT UNIVERSITY

UZ GENT

INTRODUCTION

^{18}F-FDG

- Most sensitive radiotracer in solid malignancies
- Images metabolism -> not very specific
- High amount of false-positives

PET-imaging

- Spatial resolution of max 3mm -> spatial resolutions are rapidly improving
- No current knowledge on ^{18}F-FDG-distribution on better resolutions
- Immunohistochemistry of eg. glucose-transporters is inadequate

GHENT UNIVERSITY

WHAT PRECEDED

Journal of Clinical Medicine

MDPI

Article

High-Resolution ^{18}F-FDG PET/CT for Assessing Three-Dimensional Intraoperative Margins Status in Malignancies of the Head and Neck, a Proof-of-Concept

Jens M. Debacker [1,2,3,4,*], Vanessa Schelfhout [4,5,6], Lieve Brochez [1,4,7], David Creytens [4,6,8], Yves D'Asseler [4,5,6], Philippe Deron [1,2,4], Vincent Keereman [9,10], Koen Van de Vijver [4,6,8], Christian Vanhove [4,9,11] and Wouter Huvenne [1,2,4]

- Tumoral margin assessment using a high-resolution preclinical PET/CT
- Increased uptake in regions with no pathological proof of malignancy
  - Issue: unable to correlate PET with histopathology

GHENT UNIVERSITY

Debacker, J.M. et al. High-Resolution ^{18}F-FDG PET/CT for Assessing Three-Dimensional Intraoperative Margins Status in Malignancies of the Head and Neck, a Proof-of-Concept. *J. Clin. Med.* **2021**, *10*, 3737.

LIMITATIONS

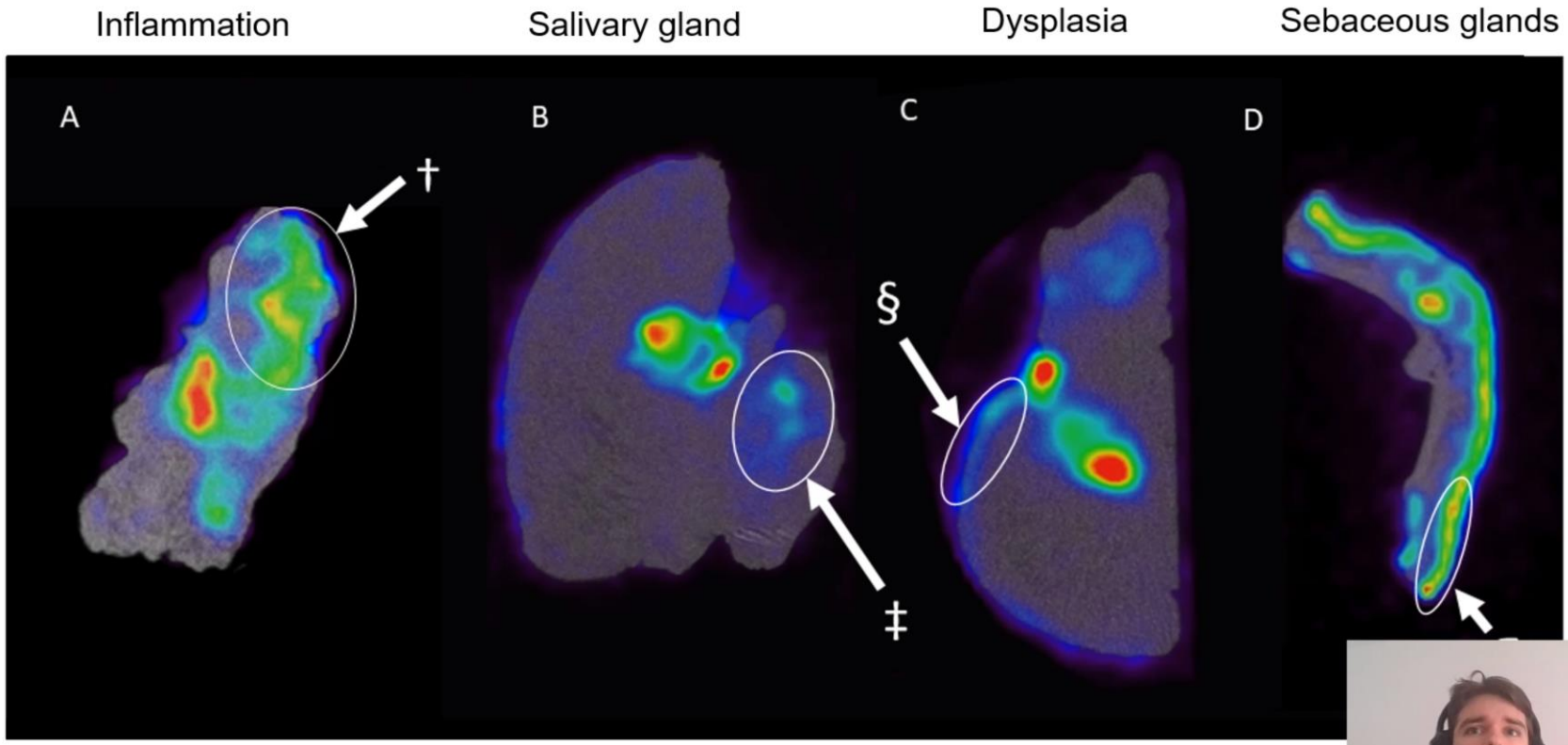

GHENT UNIVERSITY

Debacker, J.M. et al. High-Resolution ^{18}F-FDG PET/CT for Assessing Three-Dimensional Intraoperative Margins Status in Malignancies of the Head and Neck, a Proof-of-Concept. *J. Clin. Med.* **2021**, *10*, 3737.

METHODOLOGY (1)

A. ^{18}F-FDG administration & Standard of care surgery

B. µPET/CT of specimen

C. Tumor slicing

D. µPET of slices

E. Frozen sections

F. Autoradiography

G. Histopathology

H. Coregistration

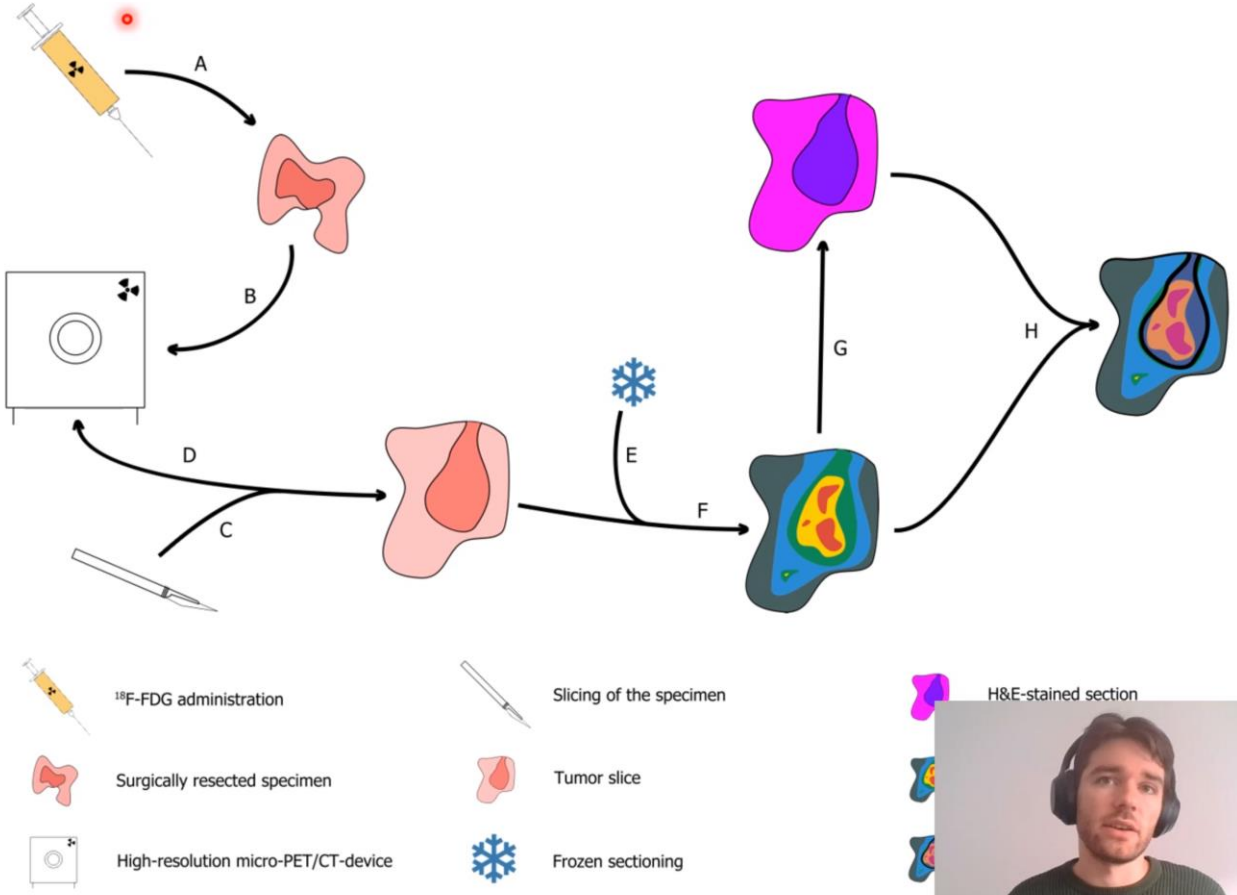

METHODOLOGY (2)

A. ^{18}F-FDG administration & Standard of care surgery

B. µPET/CT of specimen

C. Tumor slicing

D. µPET of slices

E. Frozen sections

F. Autoradiography

G. Histopathology

H. Coregistration

Example case:

- 62 year old male patient
- epithelioid angiosarcoma of the nasal tip
- Planned for nasal resection

METHODOLOGY (3)

A. ^{18}F-FDG administration & Standard of care surgery

B. µPET/CT of specimen

C. Tumor slicing

D. µPET of slices

E. Frozen sections

F. Autoradiography

G. Histopathology

H. Coregistration

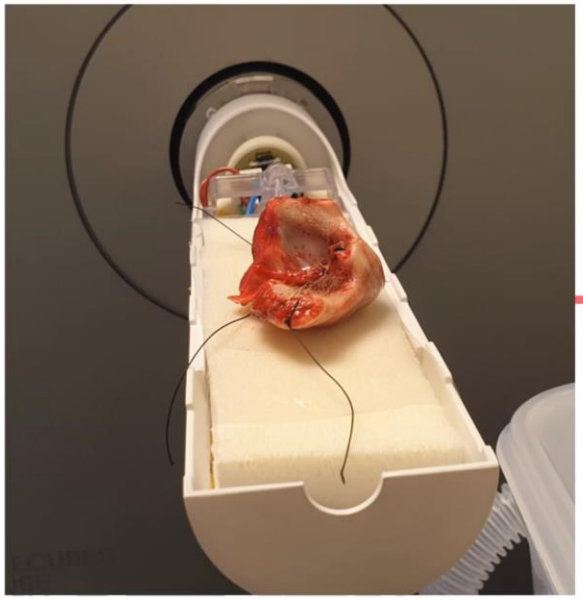

µPET/CT

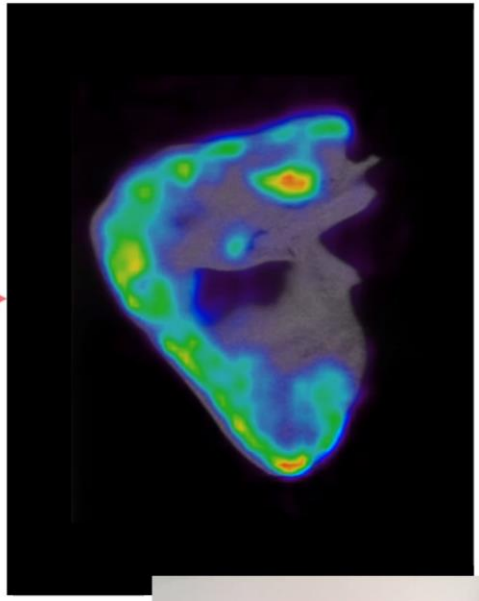

METHODOLOGY (4)

- A. ^{18}F-FDG administration & Standard of care surgery
- B. µPET/CT of specimen
- **C. Tumor slicing**
- D. µPET of slices
- E. Frozen sections
- F. Autoradiography
- G. Histopathology
- H. Coregistration

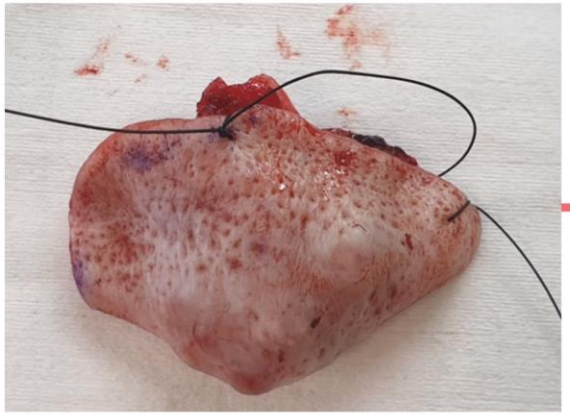

Tumor slicing

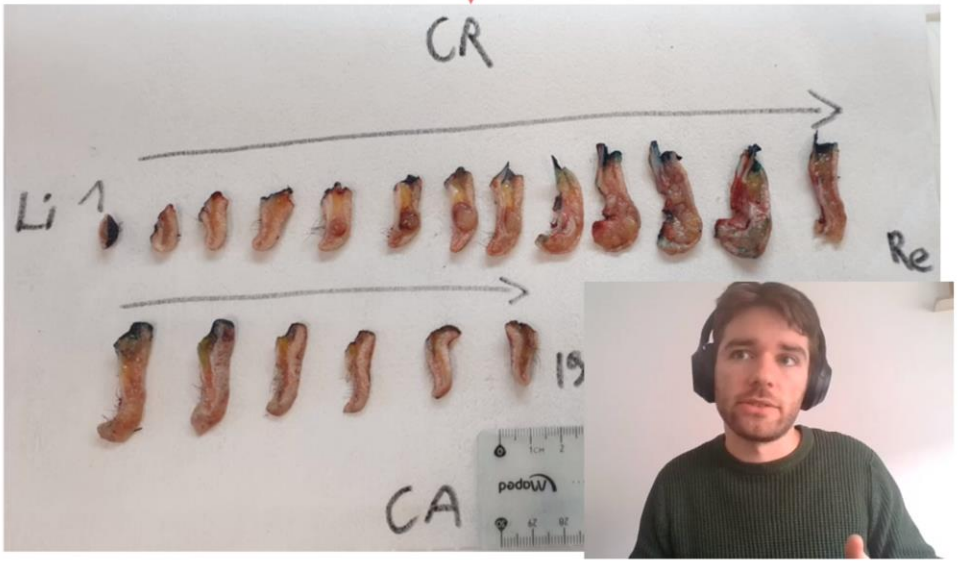

METHODOLOGY (5)

A. ^{18}F-FDG administration & Standard of care surgery

B. µPET/CT of specimen

C. Tumor slicing

D. µPET of slices

E. Frozen sections

F. Autoradiography

G. Histopathology

H. Coregistration

µPET/CT

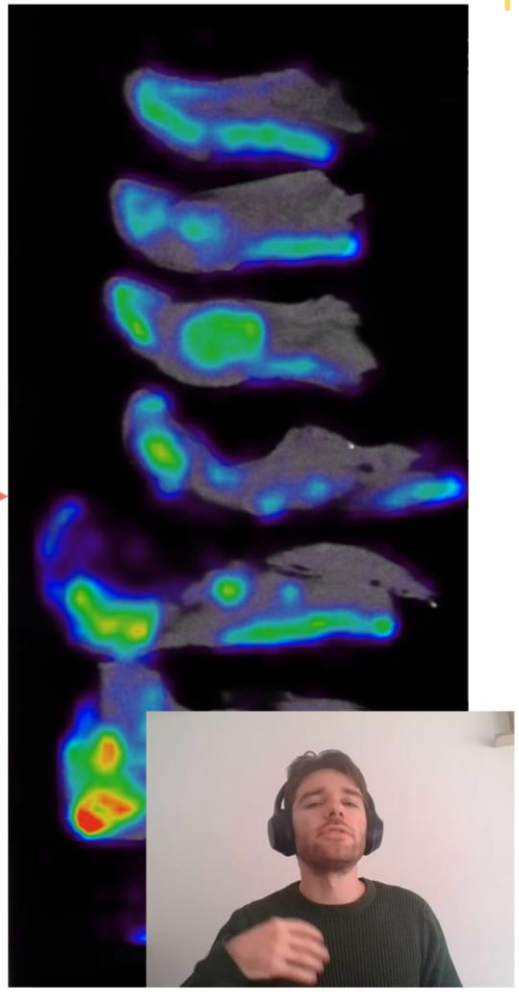

METHODOLOGY (6)

A. ^{18}F-FDG administration & Standard of care surgery

B. µPET/CT of specimen

C. Tumor slicing

D. µPET of slices

E. Frozen sections

F. Autoradiography

G. Histopathology

H. Coregistration

Frozen sectioning

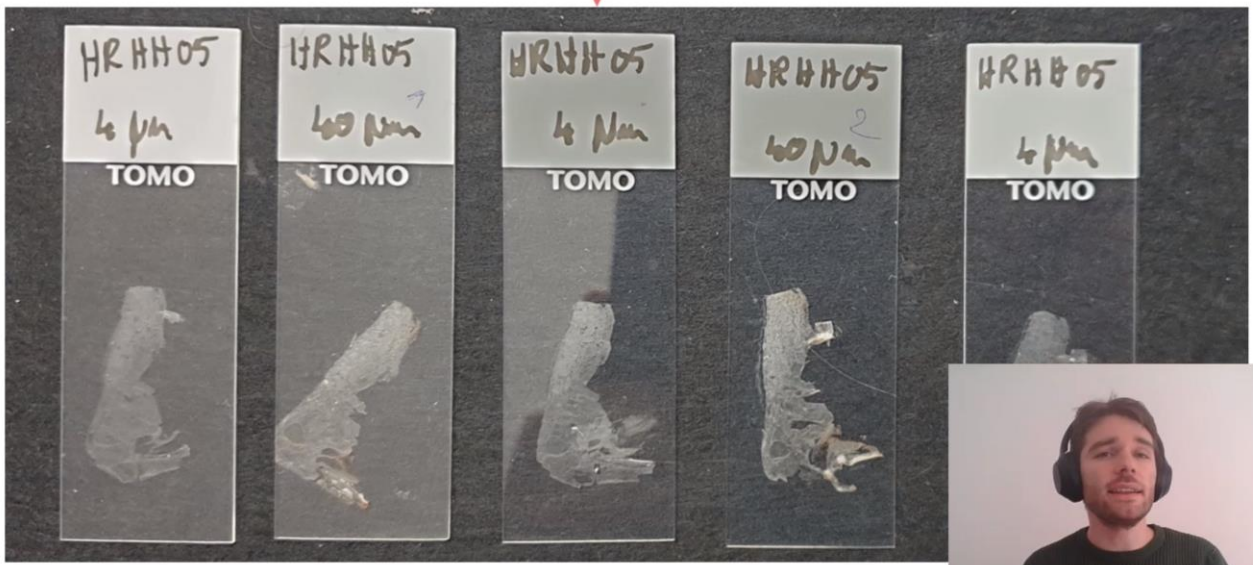

METHODOLOGY (7)

A. ^{18}F-FDG administration & Standard of care surgery

B. µPET/CT of specimen

C. Tumor slicing

D. µPET of slices

E. Frozen sections

F. Autoradiography

G. Histopathology

H. Coregistration

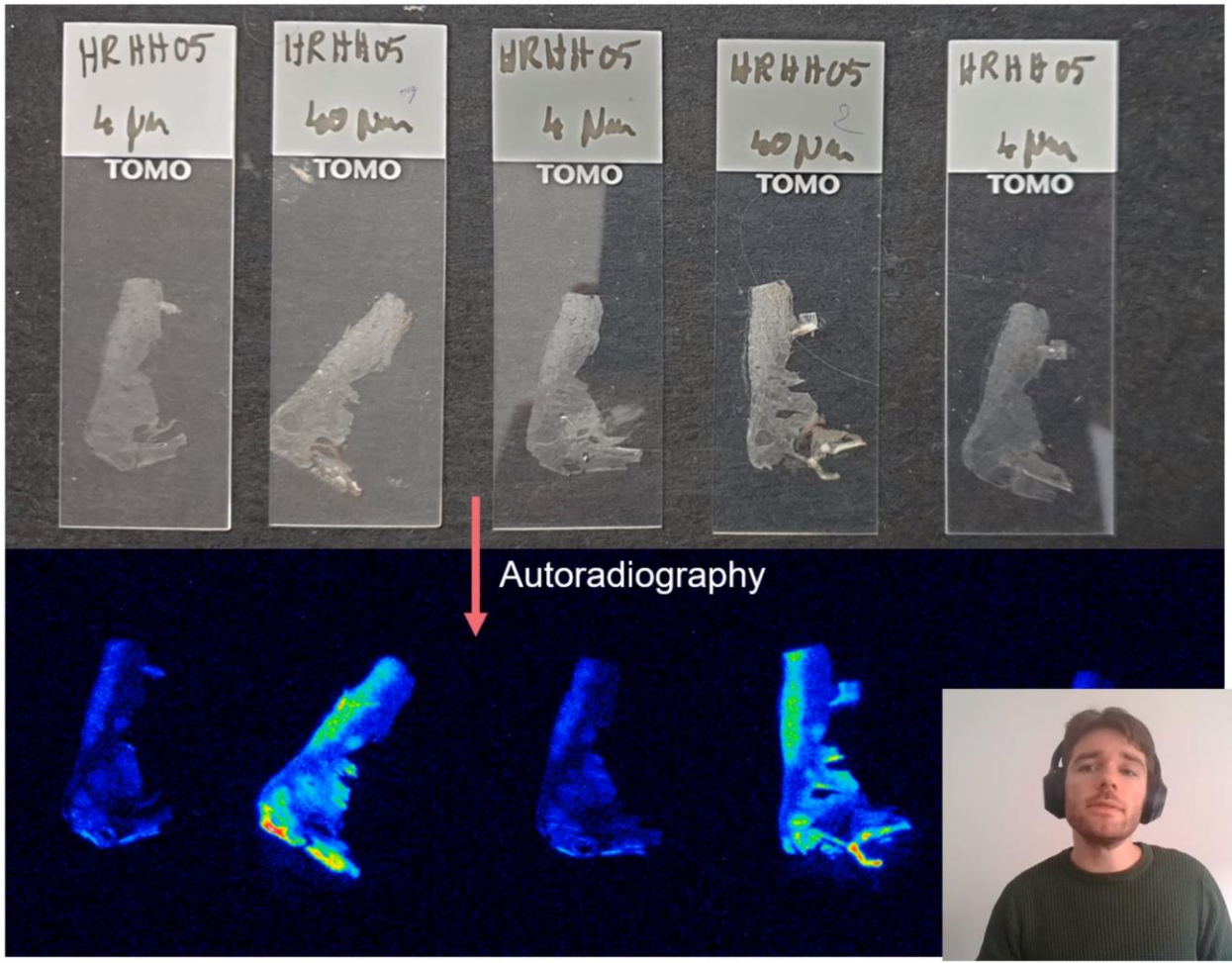

METHODOLOGY (8)

A. ^{18}F-FDG administration & Standard of care surgery

B. µPET/CT of specimen

C. Tumor slicing

D. µPET of slices

E. Frozen sections

F. Autoradiography

G. Histopathology

H. Coregistration

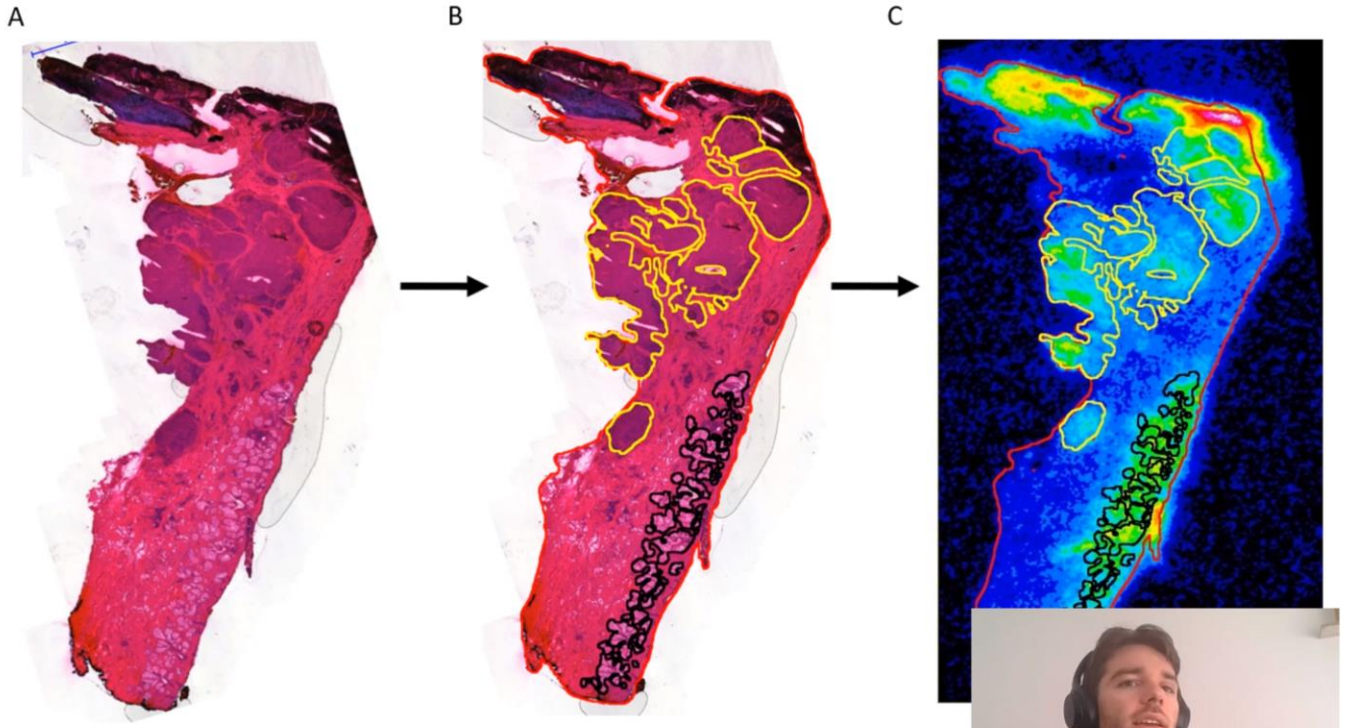

FINDINGS

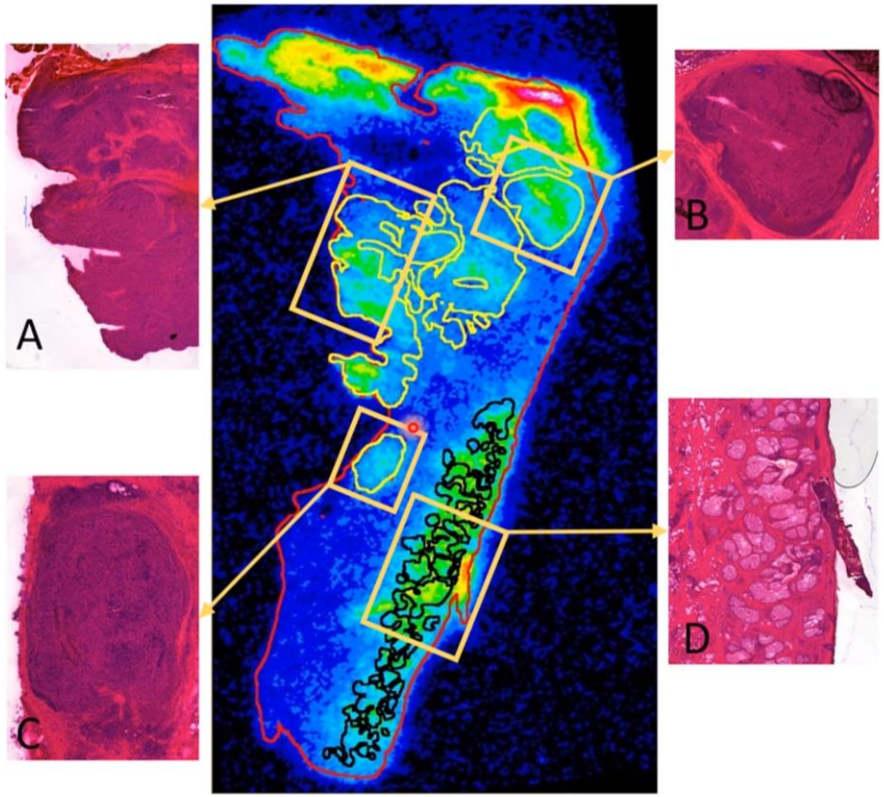

1. A previously unexplored accuracy between histopathology and autoradiography
2. Heterogeneous uptake is detected in different clusters of malignancy
3. High(er) uptake in benign inflamed tissue

GHENT UNIVERSITY

TAKE HOME MESSAGE

- Autoradiography of surgically resected specimens provides evidence of ^{18}F-FDG distribution with a **previously unprecedented accuracy**
- **Heterogeneity** of ^{18}F-FDG uptake increases with increased spatial resolution
- There is currently **no knowledge of ^{18}F-FDG-distribution** on a spatial resolution below 3-4mm

GHENT UNIVERSITY

LMU KLINIKUM
Gemeinsam. Fürsorglich. Wegweisend.

Voxel-wise correlation of amino acid and TSPO PET with relative contrast enhancement in T1-weighted MRI in gliomas

L. Kaiser[1], A. Holzgreve[1], M. Unterrainer[1,2], F. Vettermann[1], J. Brosch-Lenz[1], A. Gosewisch[1], G. Böning[1], R. Rupprecht[3], J. C. Tonn[4], P. Bartenstein[1], S. Ziegler[1], N. L. Albert[1]

[1] *Department of Nuclear Medicine, University Hospital, LMU Munich, Munich, GERMANY*
[2] *Department of Radiology, University Hospital, LMU Munich, Munich, GERMANY*
[3] *Department of Psychiatry and Psychotherapy, University of Regensburg, Regensburg, GERMANY*
[4] *Department of Neurosurgery, University Hospital, LMU Munich, Munich, GERMANY*

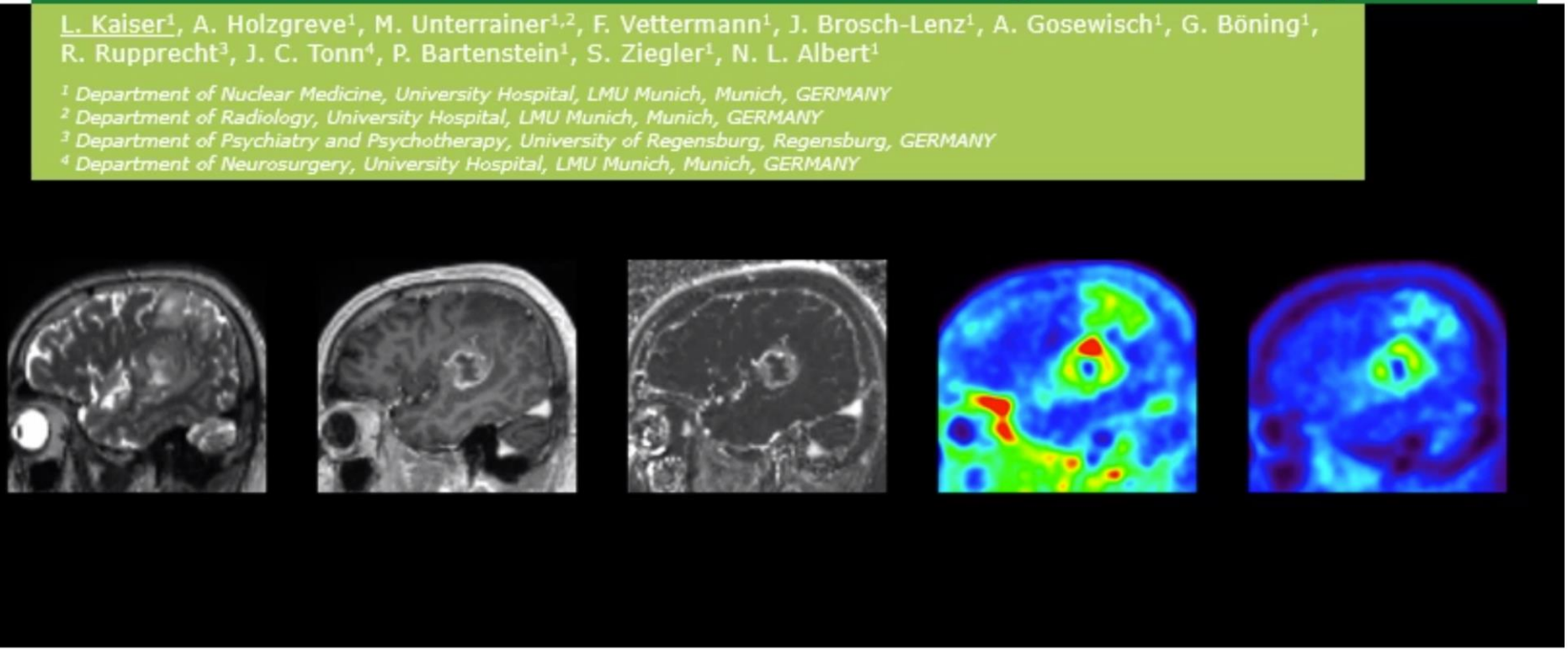

Voxel-wise correlation of multi-modal images of gliomas

Purpose

- Spatial 3D-characterisation of tumour and its micro-environment for glioma patients using **multi-modal imaging** (MRI, TSPO PET, amino acid PET)

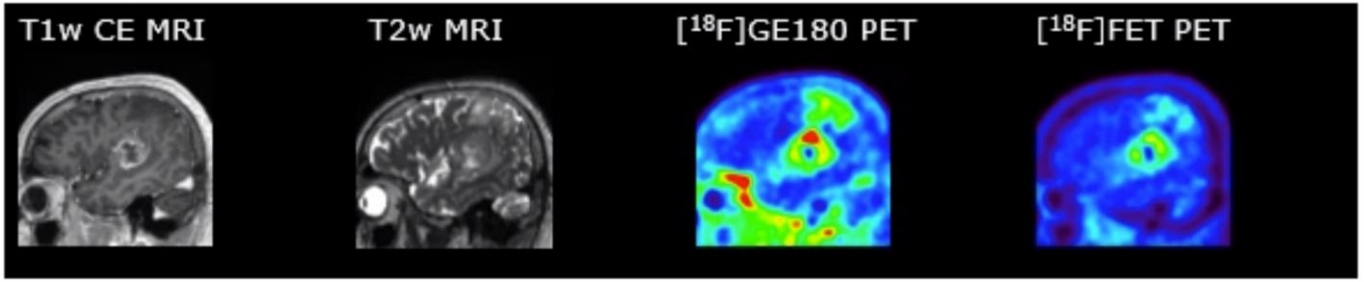

- → **Individualized treatment and improvement of prognosis**

- Goals:
  - Evaluate a potential **correlation of PET tracer uptake** with contrast-enhancement (CE) on T1w MRI
  - Assess whether PET signal is likely caused by blood brain barrier (BBB) disruption alone, or rather attributable to **specific binding after BBB passage**

Voxel-wise correlation of multi-modal images of gliomas

Dual PET data using TSPO and amino acid PET

Amino acid PET using [^{18}F]FET

- Established for non-invasive characterisation of gliomas [1, 2]
- Assumption: tumour cells exhibit increased amino acid consumption
  → elevated uptake

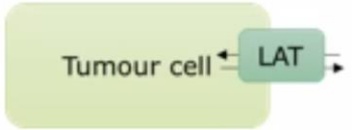

Translocator protein (TSPO) as PET target using [^{18}F]GE180

- Assumption up to now: increased expression in tumour cells & activated microglia/macrophages [3, 4]
- Recent study: increased TSPO signal in multiple sclerosis patients rather reflects a high cell density of microglial cells and not their activation phenotype [5]
- Contribution of inflammatory/tumour cells to PET signal not yet clarified
- Yet: positive correlation of TSPO PET with histologic tumour grade [6, 7] & negative correlation with patient's survival [3]

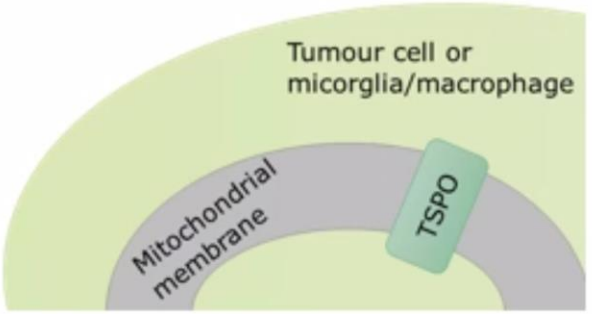

[1] Albert et al., 2016, Neuro-Oncology, DOI:10.1093/neuonc/now058
[2] Law et al. 2018, EJNMMI, DOI:10.1093/neuonc/now058
[3] Michelson et al., 2016, J Neuroimmunol 297, DOI:10.1016/j.jneuroim.2016.05.019
[4] Roesch et al., 2018, Int J Mol Sci, DOI:10.3390/ijms19020436
[5] Zinnhardt et al., 2021, Eur J Nucl Med Mol Imaging, DOI:10.1007/s00259-021-05276-5
[6] Miettinen et al., 1995, Cancer Res, https://cancerres.aacrjournals.org/content/55/12/2691
[7] Unterrainer et al., 2019, Eur J Nucl Med Mol Imaging, DOI:10.1007/s00259-019-04491-5

Voxel-wise correlation of multi-modal images of gliomas

Methods

Patients and multi-parametric imaging

- 34 patients with a suspected high-grade glioma included showing contrast enhancement on T1w MRI
- Modalities:
  - [^{18}F]FET PET
  - [^{18}F]GE180 PET
  - Contrast enhancement (CE) in T1w MRI
  - T2w MRI

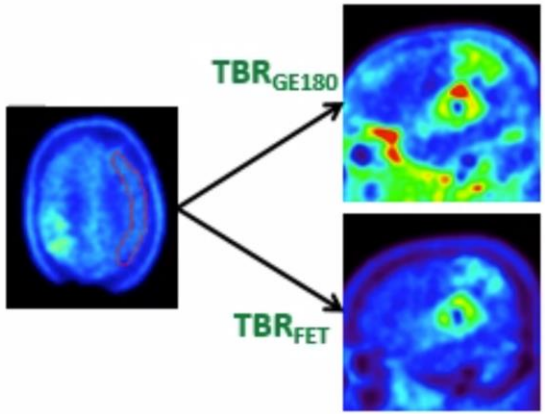

Quantification

- Static PET images: normalization using background signal (**TBR**)
- CE T1w MRI voxel values divided by native T1w MRI → relative CE (**rCE**)

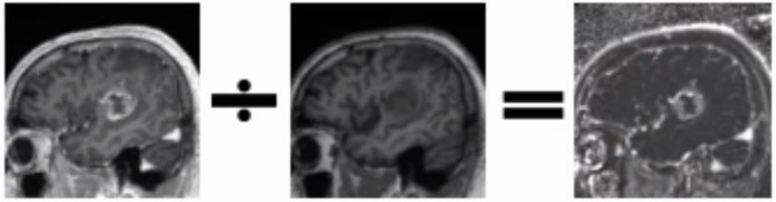

Voxel-wise correlation of multi-modal images of gliomas

Methods

Analyses:

- Voxel-wise correlation between TBR_{FET}, TBR_{GE180} & rCE
- Comparison of tumour volumes and hot-spots:
  - Spatial concordance/discordance using Dice coefficients (D)
  - Volume distance using Average Hausdorff Distance (AHD)

Segmentation:

- Whole tumour thresholds (biopsy-proven[1] or validated by two experienced physicians):
  $TBR_{GE180} > 1.8$, $TBR_{FET} > 1.6$, rCE or $TBR_{T2} > 1.3$
- Hotspots: volume corresponding to sphere with diameter of 1 cm → hottest 62 voxels
- Voxel-wise analyses: combination of whole tumour volumes including suspected areas in T2w MRI

[1] Pauleit et al. , 2005, Brain, DOI:10.1093/brain/awh399

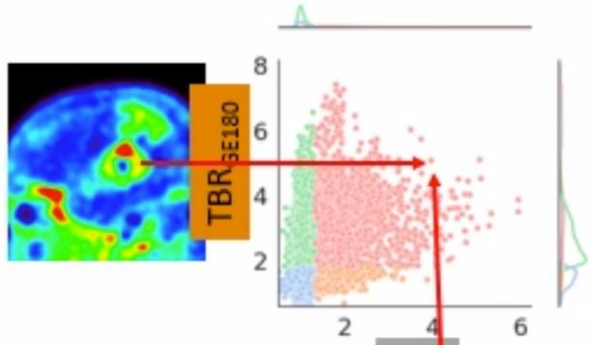

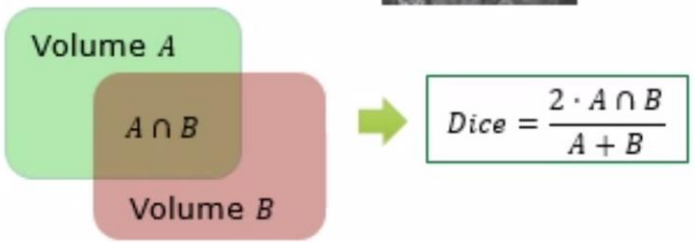

Voxel-wise correlation of multi-modal images of gliomas

Results – voxel-wise analyses

Weak correlation between TBRs and rCE

Strong correlation between TBR_{GE180} and TBR_{FET}

High PET uptake even in rCE negative areas

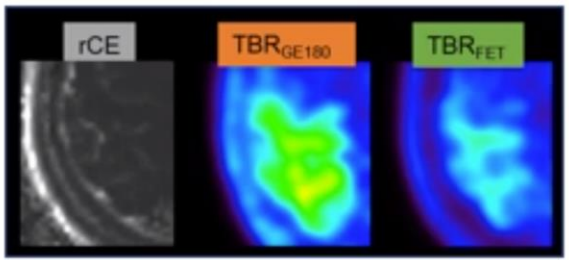

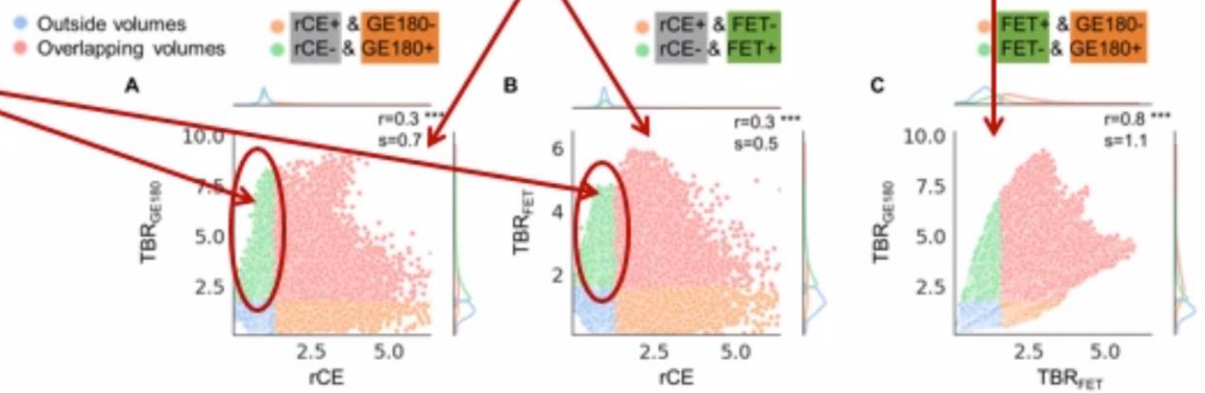

Voxel-wise correlation of multi-modal images of gliomas

Results – Dice coefficients and Average Hausdorff distances

rCE vs. TBR_{GE180} or TBR_{FET}

- No or very low overlap and large distance of hot-spots
- Moderate overlap of whole volumes

TBR_{GE180} vs. TBR_{FET}

- Low correspondence of hot-spots (12/34 with no overlap of hot-spots)
- Higher overlap of whole tumour volumes

a) Average scores for tumour hot-spots
Volume of 0.52 ml each

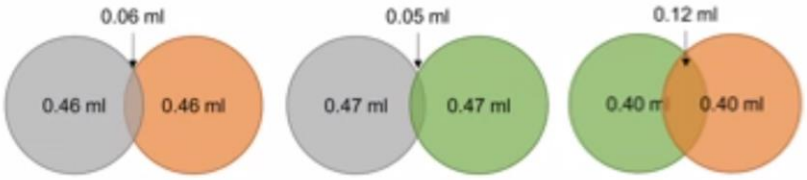

	rCE vs. TBR_{GE180}	rCE vs. TBR_{FET}	TBR_{FET} vs. TBR_{GE180}
V1 \ V2	0.46 ml (47 %)	0.47 ml (47 %)	0.40 ml (42 %)
V2 \ V1	0.46 ml (47 %)	0.47 ml (47 %)	0.40 ml (42 %)
V1 ∩ V2	0.06 ml (7 %)	0.05 ml (7 %)	0.12 ml (16 %)
Dice coefficient	11 %	10 %	23 %
Average Hausdorff distance	12.1 mm	14.3 mm	8.9 mm

b) Average scores for total tumour volumes
Volume rCE: 16 ml
Volume TBR_{FET}: 36 ml
Volume TBR_{GE180}: 47 ml

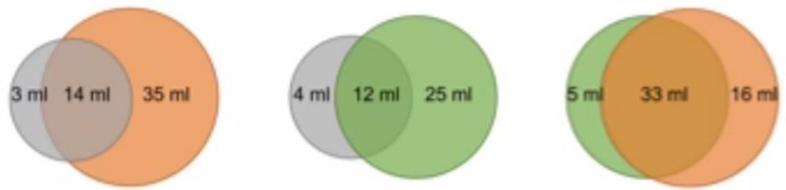

	rCE vs. TBR_{GE180}	rCE vs. TBR_{FET}	TBR_{FET} vs. TBR_{GE180}
V1 \ V2	3 ml (8 %)	4 ml (12 %)	5 ml (13 %)
V2 \ V1	35 ml (70 %)	25 ml (63 %)	16 ml (12 %)
V1 ∩ V2	14 ml (22 %)	12 ml (26 %)	33 ml (68 %)
Dice coefficient	35 %	38 %	68 %
Average Hausdorff distance	3.1 mm	2.9 mm	1.3 mm

Voxel-wise correlation of multi-modal images of gliomas

Conclusion & outlook

Conclusion

- TSPO PET, amino acid PET, and MRI provide differential information
  → interesting complementary imaging tools for an encompassing spatial glioma characterization
  → individualized therapy planning in glioma patients
- High tumor-to-background ratios in [^{18}F]GE180 and [^{18}F]FET PET images predominantly caused by specific radiotracer uptake and do not reflect BBB breakdown only

Outlook

- Evaluate differences between histologic & molecular genetic glioma classes
- Include clinically/physiologically relevant semi-quantitative or pharmacokinetic parameters from
  - Dynamic PET data
  - Dynamic DCE MRI data (e.g. perfusion, permeability)

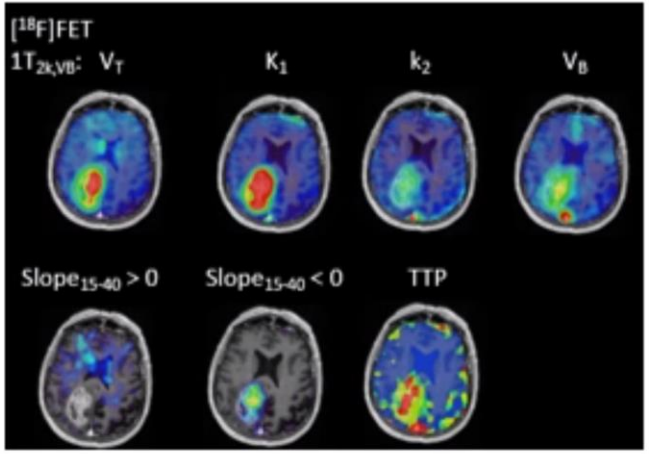

Hot needles can confirm accurate lesion sampling intraoperatively using [18F]PSMA-1007 PET guided biopsy in patients with suspected prostate cancer

Riccardo Laudicella[a,b], Daniela A. Ferraro[a,c], Konstantinos G. Zeimpekis[a], Iliana Mebert[a,d], Julian Müller[a],

Olivio F. Donati[e], Marcelo T. Sapienza[c], Jan H. Rueschoff[f], Niels J. Rupp[f], Daniel Eberli[d], Irene A. Burger[a,g]

A. Department of Nuclear Medicine, University Hospital Zurich, University of Zurich, Zurich, Switzerland

B. Nuclear Medicine Unit, Department of Biomedical and Dental Sciences and Morpho-Functional Imaging, University of Messina, Messina, Italy,

C. Department of Radiology and Oncology, Faculdade de Medicina FMUSP, Universidade de Sao Paulo, Sao Paulo, Brazil

D. Department of Urology, University Hospital Zürich, University of Zurich, Zurich, Switzerland

E. Interventional and Diagnostic Radiology, University Hospital Zurich, University of Zurich, Zurich, Switzerland

F. Department of Pathology and Molecular Pathology, University Hospital Zurich, University of Zurich, Zurich, Switzerland.

G. Department of Nuclear Medicine, Kantonsspital Baden, Baden, Switzerland

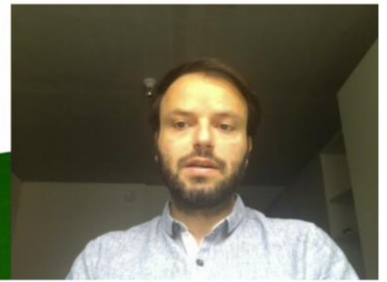

Background

PSMA PET improved the staging process of significant prostate cancer (PCa)

PSMA PET/MRI-guided fusion biopsy is promising [1]

Persisting limitation of sampling error

Purpose

To assess the possibility of intraoperative quantification of prostate-specific membrane antigen (PSMA) tracer uptake in core biopsies as an instant confirmation for accurate lesion sampling

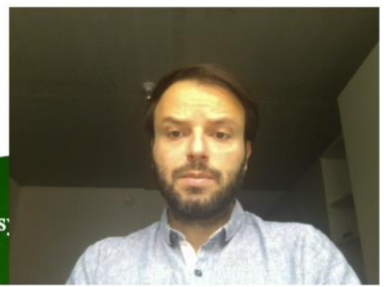

[1] Ferraro DA, Becker AS, Kranzbühler B, Mebert I, Baltensperger A, Zeimpekis KG et al. Diagnostic performance of 68Ga-PSMA-11 PET/MRI-guided biops
patients with suspected prostate cancer: a prospective single-center study. Eur J Nucl Med Mol Imaging 2021;[Epub ahead of print].

Materials and methods - Study design

Open-label, single center, non-randomized, prospective, IRB-approved study (**NCT03187990**)

Suspected PCa patients (PSA elevation > 4 ng/ml) with suspicious mpMRI lesion (PiRADS 3)

Exclusion criteria: age < 30 y or > 80 y; previous biopsy, pelvic RT, TURP, and ADT therapy; biopsy contraindications; urinary tract infections; indwelling catheter

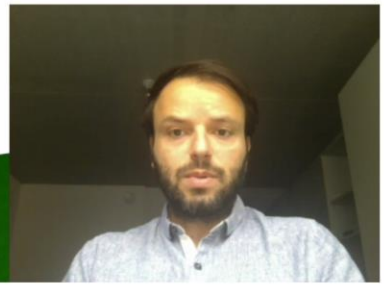

Materials and methods – Study workflow

5 patients (mean age 64.8±8.7y; mean PSA 19.7±23.5ng/ml) a mean of 51.6 days (14-169d) after mpMRI

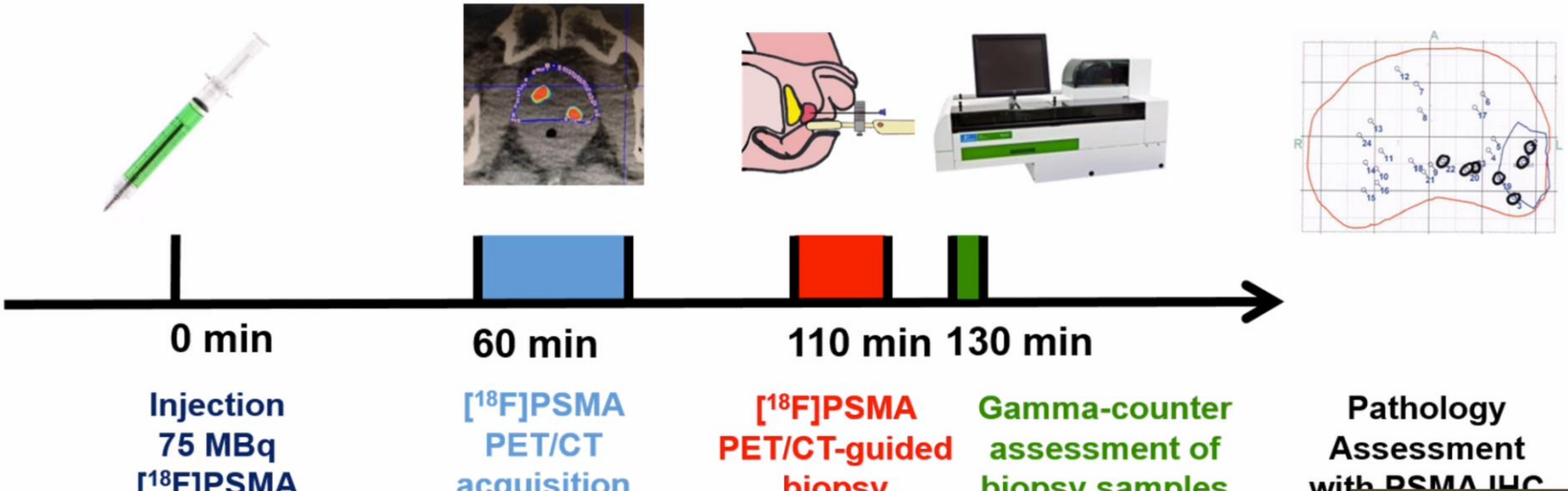

Results 43/113 cores positive for PCa

Patient	Age	PSA (ng/ml)	PiRADS	SUV_{max} (SUV_{mean})	$ISUP_{max}$ on Biopsy	Max PCa lenght (mm)*	Positive cores (n)
1	79	6.3	5	17.0 (10.3)	3	6.5	4
2	69	7	5	8.3 (4.7)	3	10.6	9
3	62	13.2	4	17.1 (9.7)	3	5	14
4	61	5.7	5	8.7 (4.7)	0	0	0
5	53	66.5	5	104.5 (59.5)	4	11	13

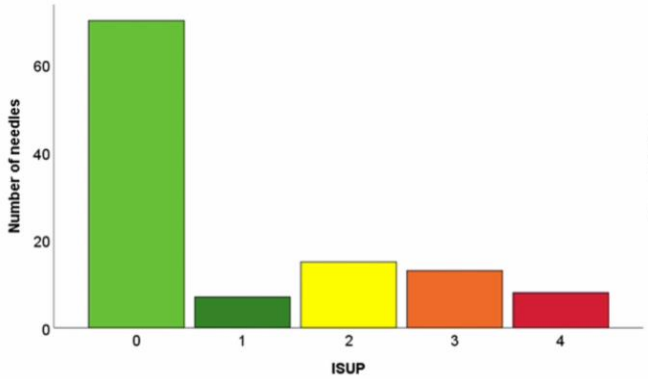

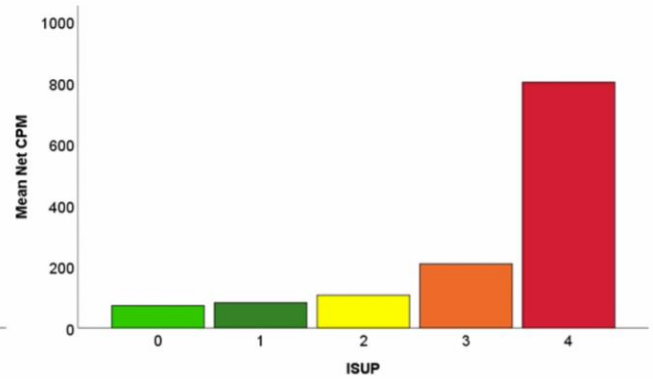

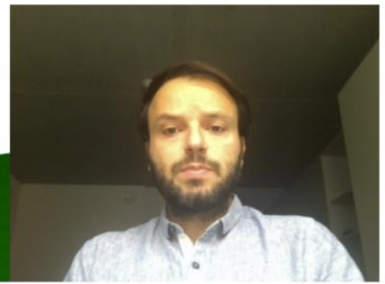

Results

In all PCa patients the 1st or 2nd PSMA-guided needle detected the highest ISUP grade of the tumor and was a **"hot needle"** with high cpm (224-2079cpm)

Patient	Needle	cpm	Gleason on first sig. PCa core (ISUP)	PCa length on first sig. PCa core (mm)	Maximum Gleason on template (ISUP)
1	First	568	4+3 (3)	6.5	4+3 (3)
2	First	156	4+3 (3)	3.2	4+3 (3)
3	Second	224	3+4 (2)	5	4+3 (3)
5	First	2079	4+4 (4)	9	4+4 (4)

43 PCa cores (97; 260±397cpm) vs **70 non-PCa cores** (64; 73±44cpm)

p<0.001

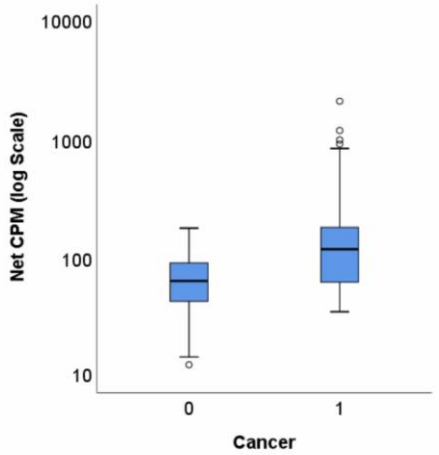

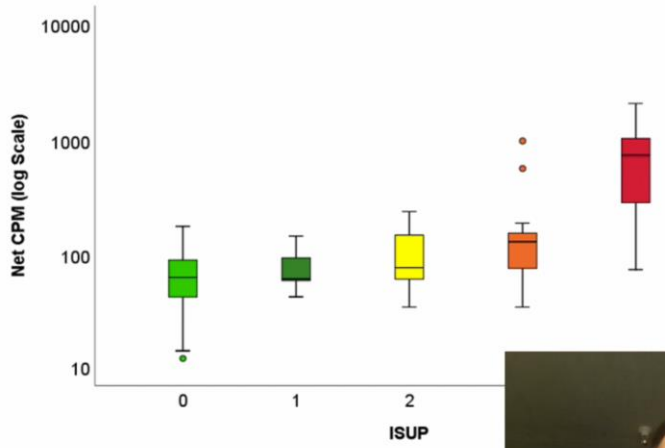

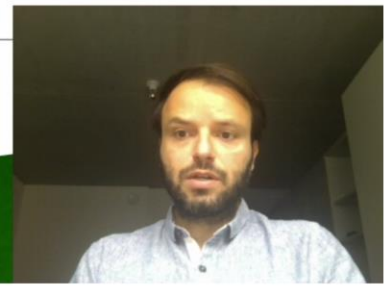

Results

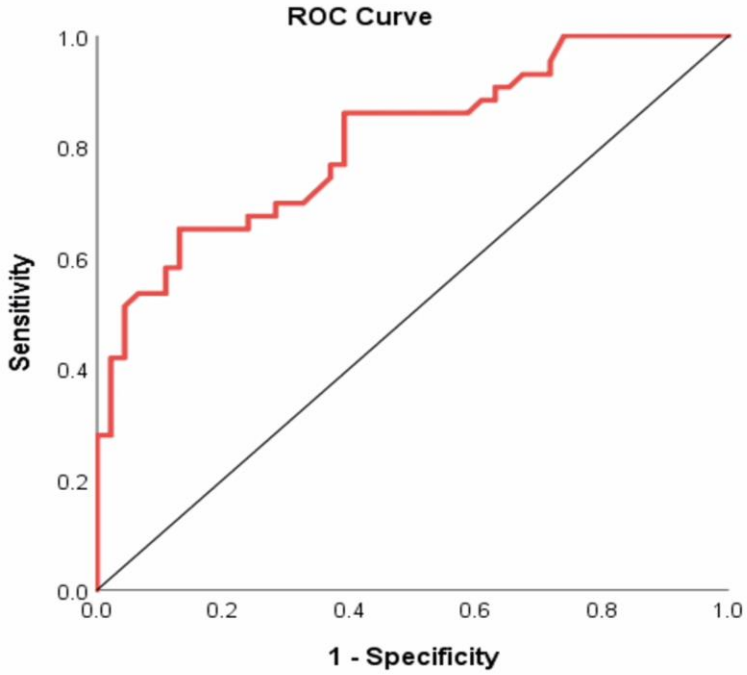

A cpm cut-off of **75** reached a ROC AUC of 0.789, with SE 65% and SP 87%

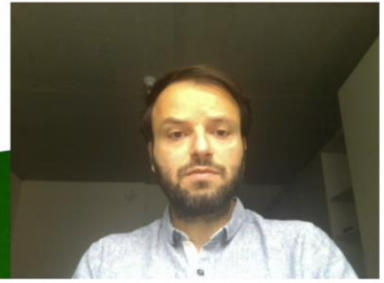

Results

61/113 cores < 75 cpm with **15/61 False Negative** at histopathology (mean core length 2 ± 2 mm)

Grade (n)	Length (mm)	PSMA membrane staining intensity	PSMA negative area	cpm
ISUP 3 (3)	2.6	2+	5%	60
	7.5	2+	60%	35
	2.1	1+	95%	38
ISUP 2 (7)	1	na	na	45
	1	1+	90%	63
	1	2+	10%	63
	6.3	1+	70%	35
	1.5	1+	40%	69
	1	na	na	61
	1.3	1+	5%	46
ISUP 1 (5)	1.5	na	na	66
	1	na	na	59
	1	na	na	43
	1	na	na	61
	1	na	na	62

52/113 cores > 75 cpm with **22/52 False Positive** at histopathology (16/22 from patient 4)

Patient (n)	PSMA membrane staining intensity	cpm
1 (2)	2+	97
	2+	91
2 (1)	3+	146
3 (1)	2+	88
4 (16)	1+	99
	nm	121
	nm	135
	1+	132
	3+	167
	2+	91
	2+	114
	2+	129
	1+	143
	1+	161
	1+	179
	1+	148
	1+	105
	1+	147
	1+	
	1+	
5 (2)	3+	
	3+	

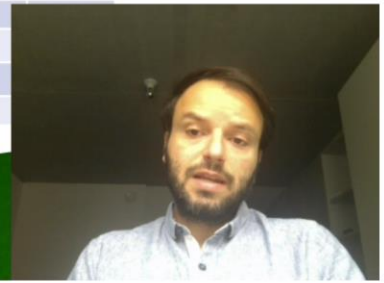

Conclusion

[18F]PSMA-1007 uptake in PCa can confirm accurate lesion sampling of the dominant tumor intraoperatively, thus improving the confidence in imaging-based biopsy guidance and eventually reduce the need for saturation biopsy.

Grazi

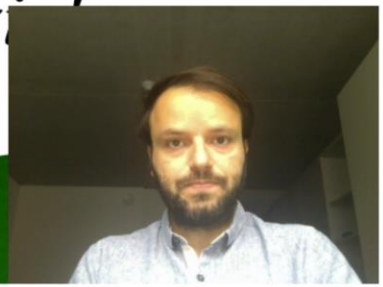


ACCREDITED PET/CT CENTRE
•2021•
RESEARCH4LIFE
an EANM initiative
OF EXCELLENCE

RESEARCH4LIFE

Amsterdam UMC
University Medical Centers

PET Harmonisation Beyond EARL
The future of EARL

Ronald Boellaard

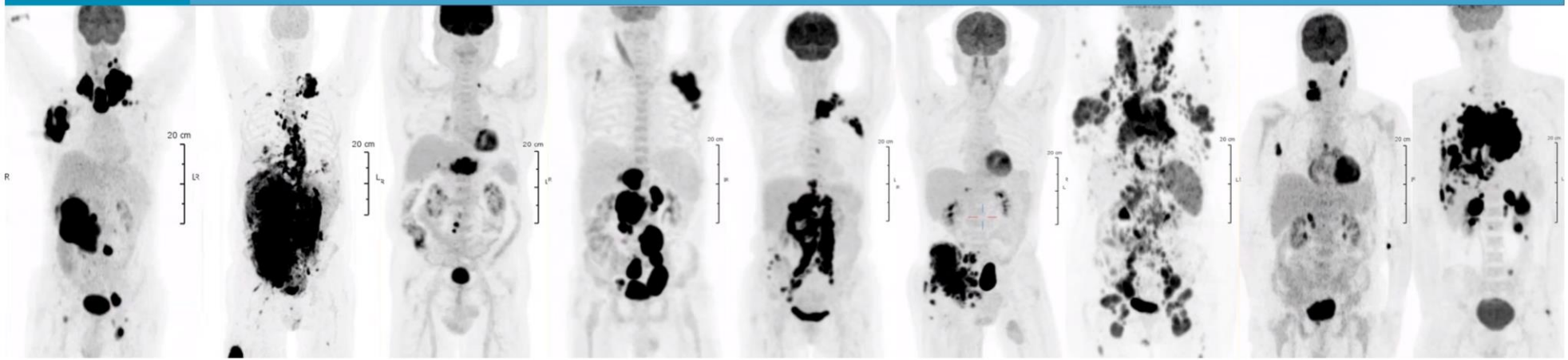

Introduction - PET/CT uncertainties[1]

$$SUV_{TBW} = \frac{c_t\,[kBq/ml]}{Dose[MBq]/weight[kg]}$$

Technical factors
- Relative calibration between PET scanner and dose calibrator (10%)
- Residual activity in syringe (5%)
- Incorrect synchronization of clocks (10%)
- Injection vs calibration time (10%)
- Quality of administration (50%)

Physics related factors
- Scan acquisition parameters (15%)
- Image reconstruction parameters (30%)
- Use of contrast agents (15%)
- ROI (50%)

Biological factors
- Uptake period (15%)
- Patient motion and breathing (30%)
- Blood glucose levels (15%)
- Changes in blood clearance

1. R. Boellaard 2009, J Nucl Med Supplement Issue 50: 11S

Guidelines and standards

- A guideline, such as the EANM guideline, provides recommendations on how to perform an imaging study (int his case FDG PET/CT):
  - patient preparation
  - acquisition
  - image interpretation & analysis
  - reporting

- What about PET/CT system performances?
- a (quantitative) read also depends on the PET/CT system performance

EARL: PET/CT accreditations in practice

1. ^{18}F standards 1 & 2, ^{89}Zr, ^{68}Ga

2. Calibration QC using uniform cylinder

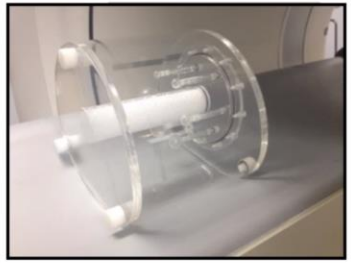

3. Image Quality QC using NEMA IEC body phantom with 6 spheres with target to background ratio of 10:1

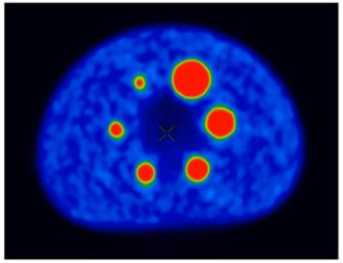

Realistic/EARL

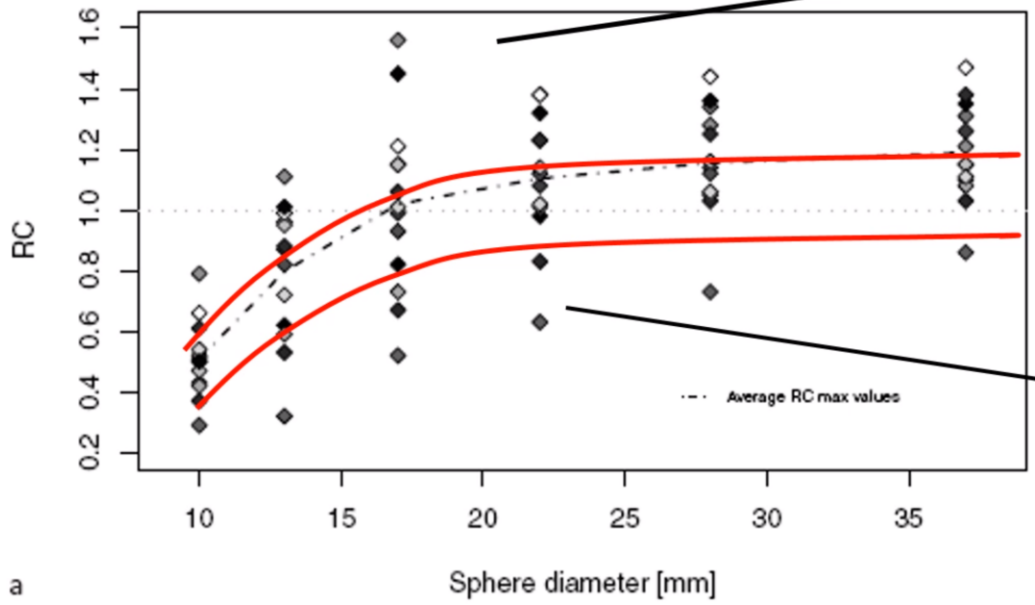

"Higher" SUVs are not necessarily 'better'

Centered at 1.0

Not defined by lowest denominator !

EARL ^{18}F-FDG PET/CT accreditation

- EARL set up the EARL FDG-PET/CT accreditation program, launched in July 2010
- Past → EARL ^{18}F standards 1 accreditation
- Present -> EARL standards 2

Introduction - new reconstructions

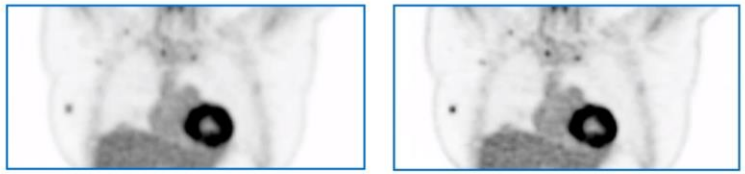

Conventional reconstruction

PSF reconstruction

- PET image reconstruction with point spread function (PSF) modelling aims to,
  - Improve spatial resolution.
- PSF images are being widely used for,
  - Visual assessment.
  - SUV quantification.

- However, prior studies have shown SUV quantification from PSF images is not directly comparable to conventional non-PSF images.

EARL 2: New technologies, standards and SUVpeak

- Prospective independent test data from 23 imaging sites
- Majority of results fit within prototype EARL specifications

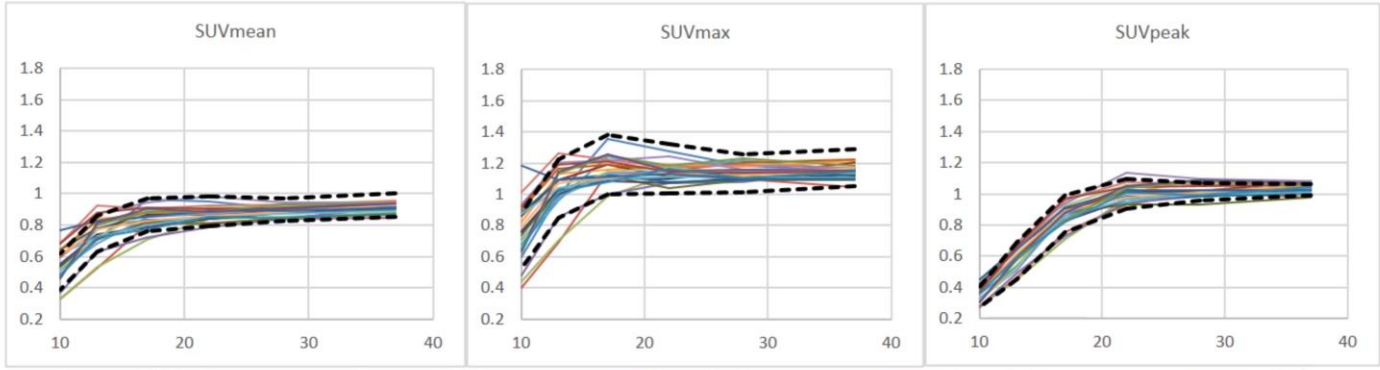

Martini Ziekenhuis
umcg
VUmc
JOHNS HOPKINS UNIVERSITY
RESEARCH 4 LIFE
an EANM initiative
Cancer Center Amsterdam

EARL ^{18}F-FDG PET/CT accreditation

- EARL set up the EARL FDG-PET/CT accreditation program, launched in July 2010
- Past → EARL ^{18}F standards 1 accreditation
- Present -> EARL standards 2
- Future -> ^{89}Zr, ^{68}Ga

^{89}Zr and ^{68}Ga - principles

- For these isotopes ‘only’ the positron emissions are seen by the PET/CT systems (non-prompts gamma are not detected) – NB this is not the case for 124I

- Reconstruction setting that harmonizes for 18F also harmonizes (differently) for 89Zr and 68Ga – only impact of positron range – thus somewhat lower SUV recoveries

^{89}Zr – isotope used for antibody labelling

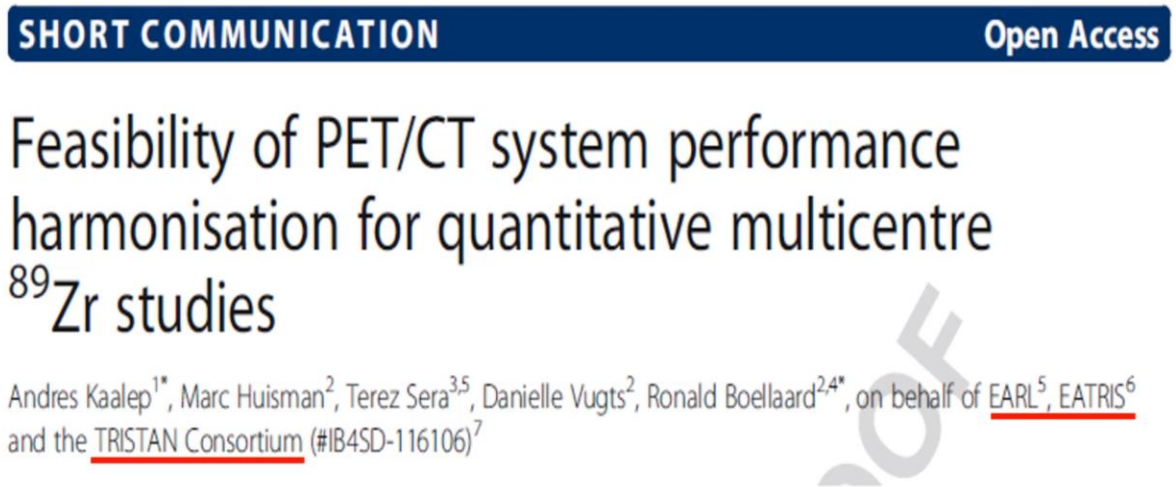

SHORT COMMUNICATION Open Access

Feasibility of PET/CT system performance harmonisation for quantitative multicentre ^{89}Zr studies

Andres Kaalep[1*], Marc Huisman[2], Terez Sera[3,5], Danielle Vugts[2], Ronald Boellaard[2,4*], on behalf of EARL[5], EATRIS[6] and the TRISTAN Consortium (#IB4SD-116106)[7]

^{89}Zr PET accreditation

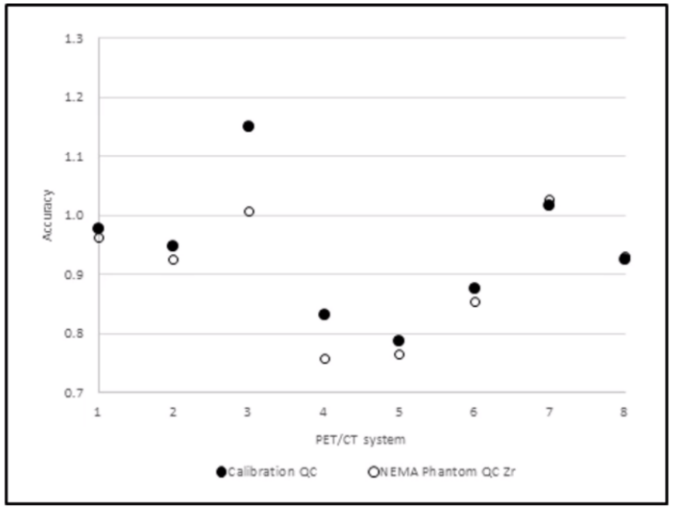

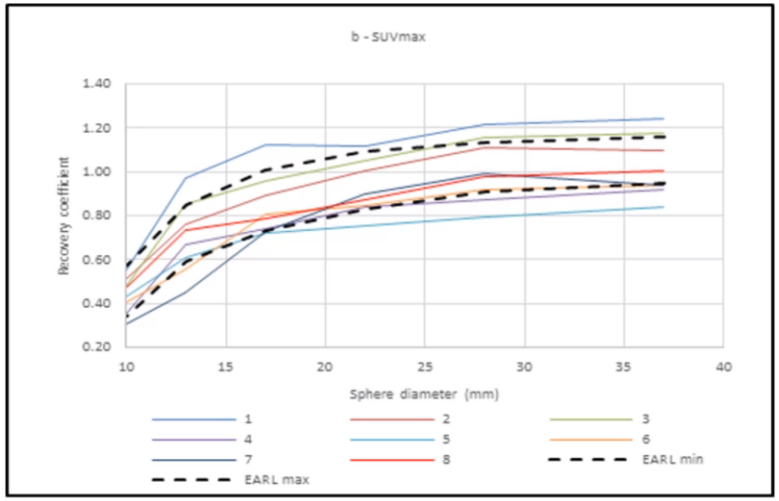

4 out of 8 systems show a calibration error of more than 10%

^{89}Zr recovery curves are comparable to those seen with FDG (apart from the calibration error)

^{68}Ga PET accreditation

- For ^{68}Ga almost the same procedure will be performed as for ^{89}Zr
- Prerequisite is 18F standards **2**

Huizing *et al. EJNMMI Physics* (2019) 6:19
https://doi.org/10.1186/s40658-019-0253-z

EJNMMI Physics

SHORT COMMUNICATION Open Access

Multicentre quantitative ^{68}Ga PET/CT performance harmonisation

Daphne M. V. Huizing[1], Daniëlle Koopman[2], Jorn A. van Dalen[3], Martin Gotthardt[4], Ronald Boellaard[5,6,7], Terez Sera[7], Michiel Sinaasappel[8], Marcel P. M. Stokkel[1] and Berlinda J. de Wit-van der Veen[1*]

Future EARL accreditations

- Brain (under evaluation)
- SPECT (under evaluation)

Amsterdam UMC
Universitair Medische Centra

Harmonisation of PET/CT Performance for Brain Studies

E.E. Verwer, S.V.S. Golla, A. Kaalep, M. Lubberink, F.H.P. van Velden, V. Bettinardi, M.M. Yaqub, T. Sera, S. Rijnsdorp, A.A. Lammertsma, R. Boellaard.

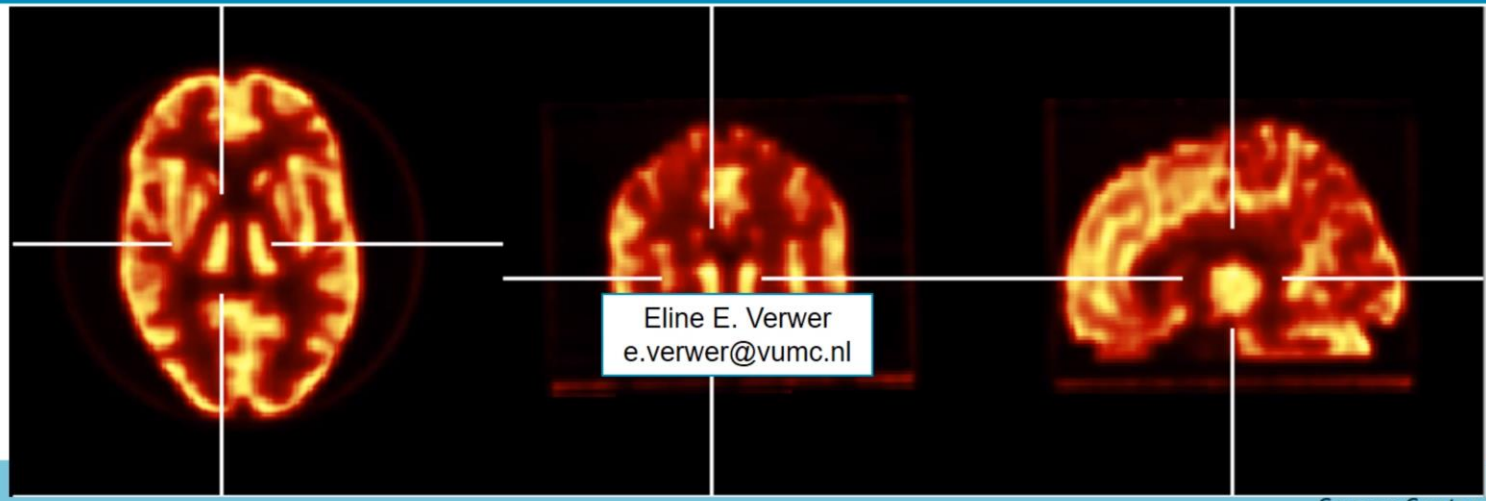

Eline E. Verwer
e.verwer@vumc.nl

Cancer Center Amsterdam

Harmonisation by COMBAT[1]

- Combat is a data-driven transformation that aligns the distribution of data

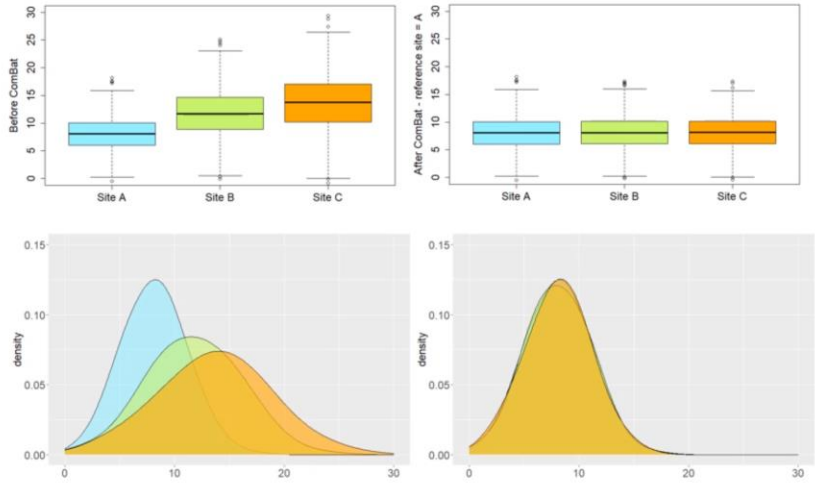

- Requires n=20 to 30 large datasets that are comparable across sites and/or needs to be used with covariates[1]

1. *A guide to ComBat harmonization of imaging biomarkers in multicenter studies, Orlhac et al, JNM (under review)*

	Upfront harmonization (like EARL)	ComBat
Opportunities	• Applicable without restriction on the number of patients • Valid for any pathology and feature - high generalizability	• Applicable directly on the calculated radiomic feature values (no need to access or reanalyze images) • No need for phantom acquisition • Applicable retrospectively • Applicable prospectively if data have already been acquired for the same pathology with the same acquisition and analysis protocols and settings • Ability to realign data to a particular site
Limitations	• Not applicable retrospectively • Requires acquisition of phantom images, optimization of reconstruction settings and access to the machine	• Minimum number of patients is needed to estimate transformation (~20-30 patients per batch) • Specific transformation for each type of tissue, each type of tumor, each scanner, each material in a phantom, each analysis method (e.g., segmentation approach) and each feature - low generalizability • Not applicable prospectively if little or no previously acquired data


ACCREDITED PET/CT CENTRE
•2021•
RESEARCH4LIFE
an EANM initiative
OF EXCELLENCE

Houses of Parliament, St Thomas's Hospital and the London Eye

Biomarkers in Lymphoma: PET for prognosis and response prediction

Sally Barrington

NIHR Research Professor of PET Imaging

Kings College London and Guy's and St Thomas' PET Centre, U

NHS
National Institute for Health Research

Prognosis

- PET-CT recommended for staging of FDG-avid lymphomas [1,2]
- Based on superior staging accuracy compared with CT
- PET alters management in up to 20-25% patients [3-5]
- Baseline provides map for response evaluation
- More accurate staging → better informed treatment choices and clinical decision making

[1]Barrington SF et al JCO 2014; 32: 3048-58, [2]Cheson BD et al JCO 2014; 32: 3059-3068,
[3]Barrington SF et al Blood 2016; 127: 1531-8, [4]Raanani P et al Ann Oncol 2006; 17: 117-122,
[5]Le Dortz et al EJNMMI 2010; 37: 2307-2314

Prognosis: Disease burden

MTD

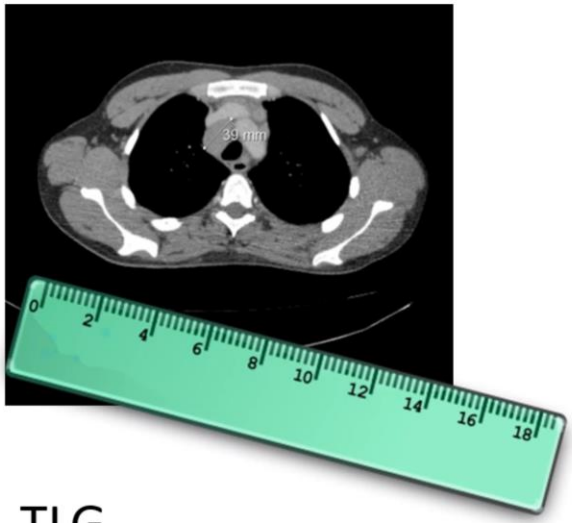

MTV

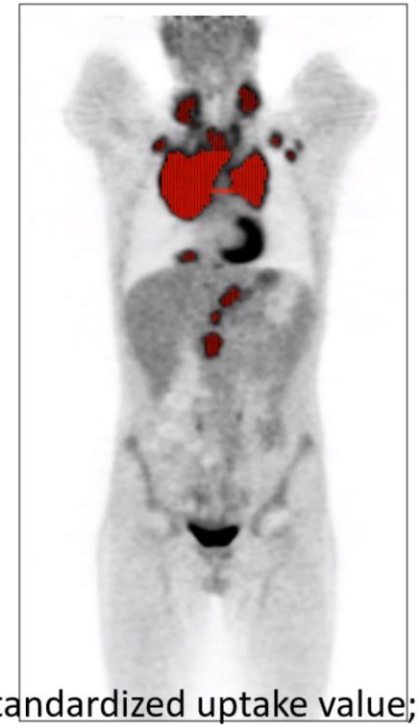

TLG

MTV x mean SUV in total volume

MTD/V: metabolic tumour diameter/volume; SUV: standardized uptake value; TLG: total lesion glycolysis.

DLBCL Disease dissemination - Dmax

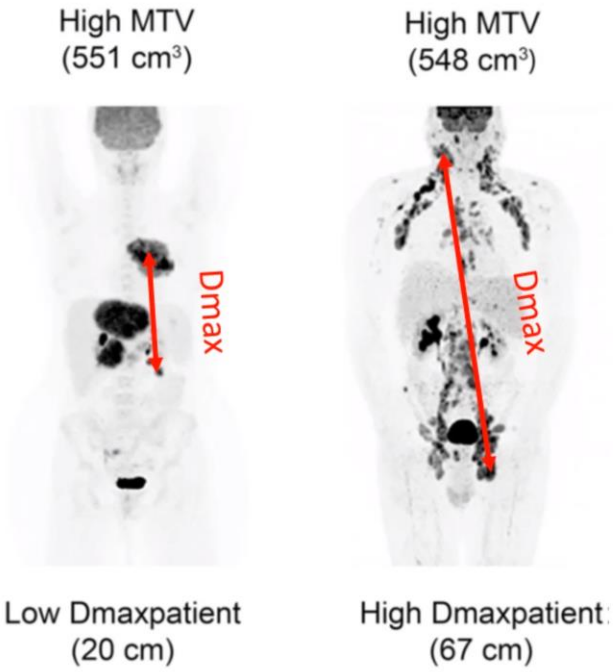

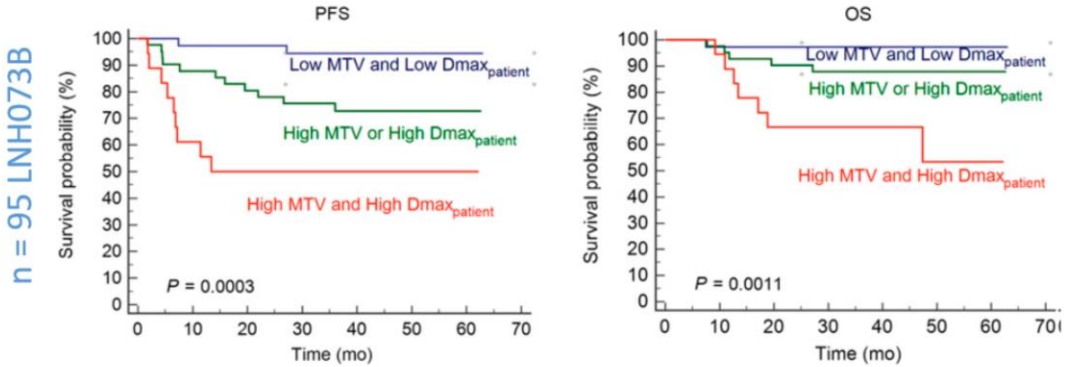

Cottereau AS et al J Nucl Med 2020; 61: 40-45

Heterogeneity

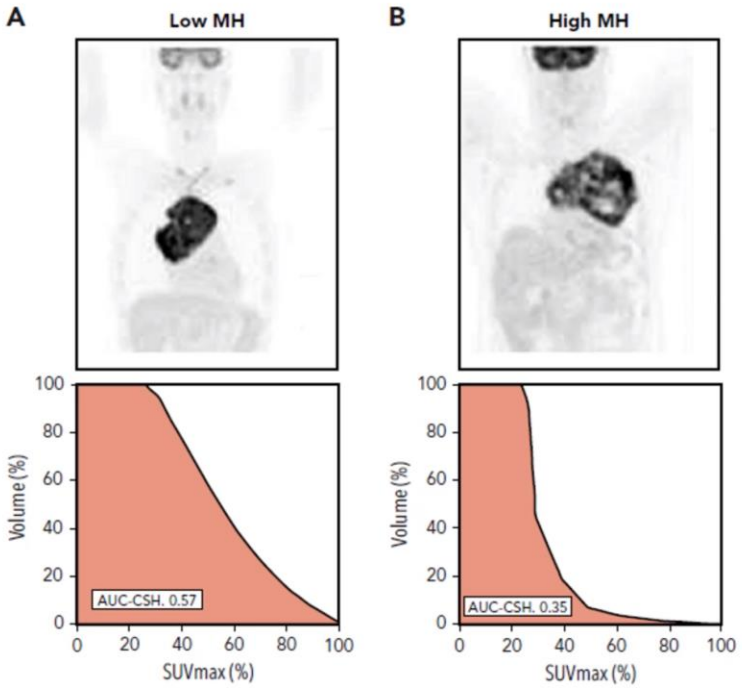

PMBCL n = 103 [1]

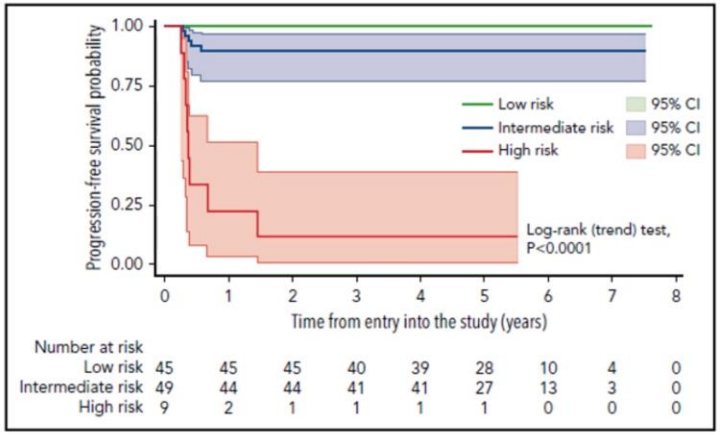

DLBCL n = 113 [2]

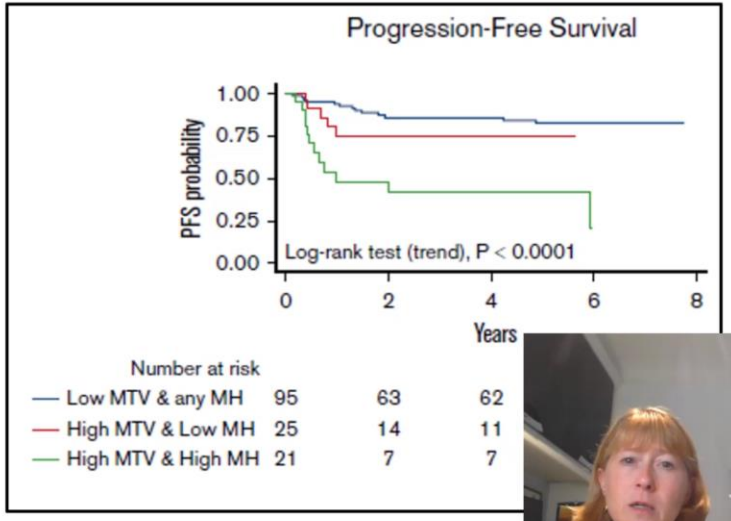

[1]Ceriani L et al Blood 2018; 132: 179-186

[2]Ceriani L et al Blood Advances 2020; 4: 1082-92

DLBCL 60-80 years : subcutaneous fat density

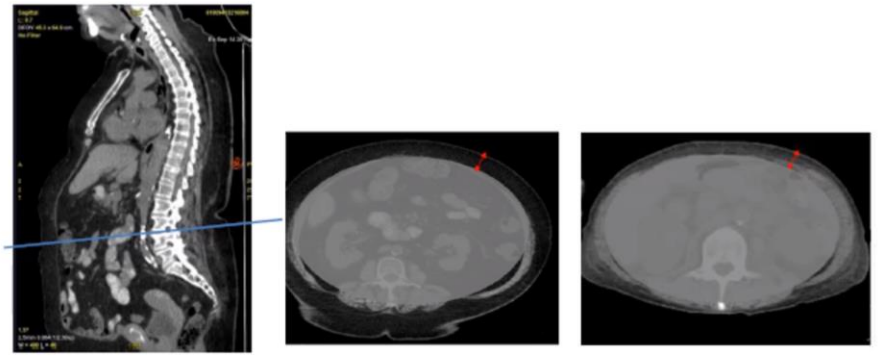

Subcutaneous Fat at L3

Low density < 90HU

High density ≥ 90HU

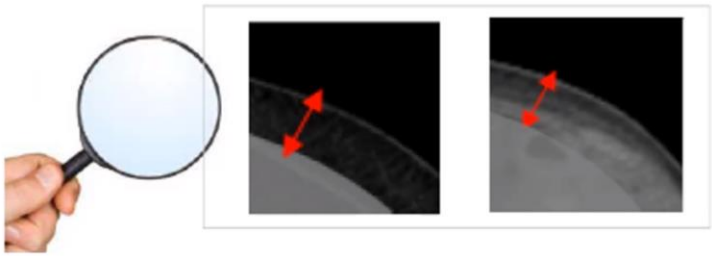

n = 273 REMARC 60-80y

c/o Pr C Thieblemont, ICML 2021 Lugano abstract 17

	ACCREDITED PET/CT CENTRE •2021• RESEARCH4LIFE an EANM initiative OF EXCELLENCE		
			

The role of ^{18}F-FDG PET/CT for evaluating immunotherapy response in patients with NSCLC: a systematic review and meta-analysis

Reporter: Mingxing Huang

Correspondence to: Prof. Rong Tian

From Department of Nuclear Medicine,West China Hospital, Sichuan University, Sichuan; China

background

biomark

ers

Three main types of imaging biomarkers can be extracted from 18F-FDG PET: tumor burden (MTV, TLG), tumor glucose uptake (SUVmax, SUVmean), and nontumoral hematopoietic tissue metabolism.

Prior studies had noted a prognostic value of SUVmax, as is commonly used in clinical practice. Jun Im et al. postulated that total lesion glycolysis (TLG) and metabolic tumor volume (MTV) were better predictors of treatment outcomes than SUVmax and SUVmean in lung cancer patients undergone surgery, chemotherapy, or radiotherapy.

Methods

STEP1

MEDLINE, PubMed, Cochrane, Scopus, Embase, and Web of Science databases were searched until April 25, 2021.

STEP2

The search strategy was based on the combination of the following keywords: immune checkpoint inhibitor OR immunotherapy", "non-small-cell lung cancer OR NSCLC", "18F-FDG OR positron emission tomography", AND "response OR prognostic OR survival". We also screened the references of the included articles to identify additional eligible studies.

STEP3

Inclusion criteria were: patients with advanced NSCLC, received immunotherapy, undergone FDG-PET scan before the start of the treatment. Detailed data were extracted and categorized.

STEP4

We used the hazard ratios of SUVmax, SUVmean, MTV, and TLG on overall survival (OS) and progression-free survival (PFS) to assess the outcome metrics. Comprehensive meta-analysis software was used for analysis.

results

Table 5. The outcomes of WMD of SUVmax, TLG and MTV

Outcomes	Number	WMD	95%CI	P	I2
SUVmax	4	3.65	-1.345-10.445	0.292	82.7
TLG	3	-143.802	-341.221-53.617	0.153	0
MTV	4	-36.273	-60.051-12.495	0.003	0

Among the above parameters, only MTV could distinguish the difference between responders and non-responders (P=0.003). We reviewed several studies to compare traditional and modified PET-based response criteria and found that PET-based criteria could be more reliable in predicting the response.

results

Table3. HRs and *p* values of individual studies and pooled data of SUVmax, SUVmean MTV and TLG for PFS and OS.

PFS/Outcomes	Number	HR	LL-UL	P	I2
SUVmax	3	0.685	0.497-0.979	0.038	0.00%
SUVmean	2	0.481	0.298-0.774	0.003	0.00%
MTV	3	0.909	0.396-2.085	0.822	84.00%
TLG	2	0.444	0.274-0.72	0.001	0.00%
OS/Outcomes					
SUVmax	3	0.753	0.486-1.167	0.204	0.00%
SUVmean	2	0.456	0.224-0.927	0.03	0.00%
MTV	3	1.217	0.2-5.401	0.796	86.80%
TLG	2	0.472	0.128-1.739	0.259	53.40%

Based on the baseline ^{18}F-FDG PET/CT imaging, the pooled hazard ratios (HRs) of SUV_{max}, SUV_{mean}, MTV and TLG for OS and PFS on this table.

conclusions

The baseline ^{18}F-FDG PET/CT parameters of SUV_{max}, SUV_{mean}, MTV, and TLG are effective in predicting the final response to immunotherapy in NSCLC patients. MTV appears to be associated with tumor response rather than the intensity of ^{18}F-FDG uptake. The immunotherapy-modified response assessment criteria are potentially an appropriate method for monitoring immunotherapy.

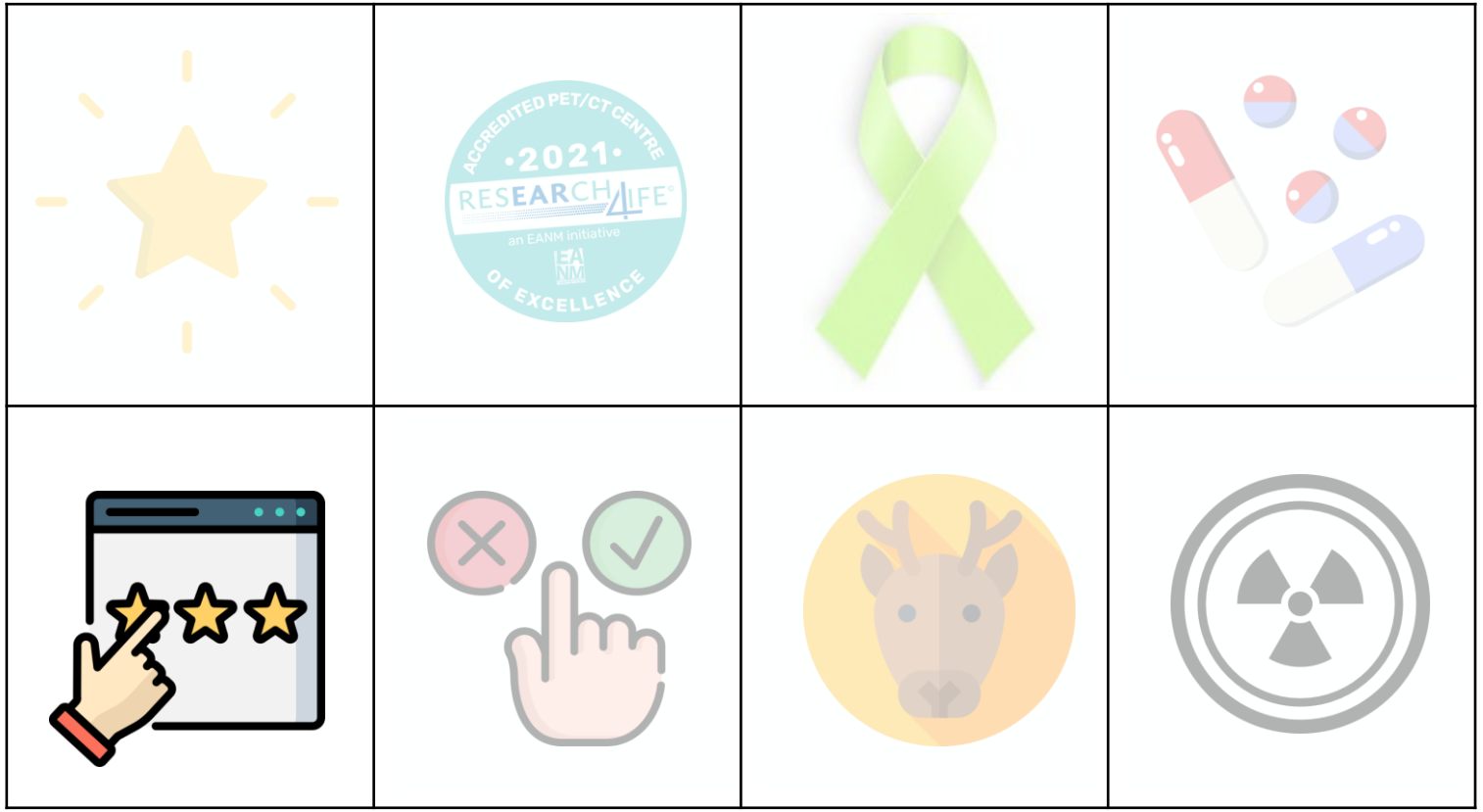
ACCREDITED PET/CT CENTRE
•2021•
RESEARCH4LIFE
an EANM initiative
OF EXCELLENCE

Amsterdam UMC
University Medical Centers

Cancer Center Amsterdam

A simulation study to compare cross-validation versus holdout or external testing to assess the performance of machine learning based clinical prediction rules

R. Boellaard, J.J. Eertink, P.J. Lugtenburg, G.J.C. Zwezerijnen, S.E. Wiegers, H.C.W. de Vet, J.M. Zijlstra

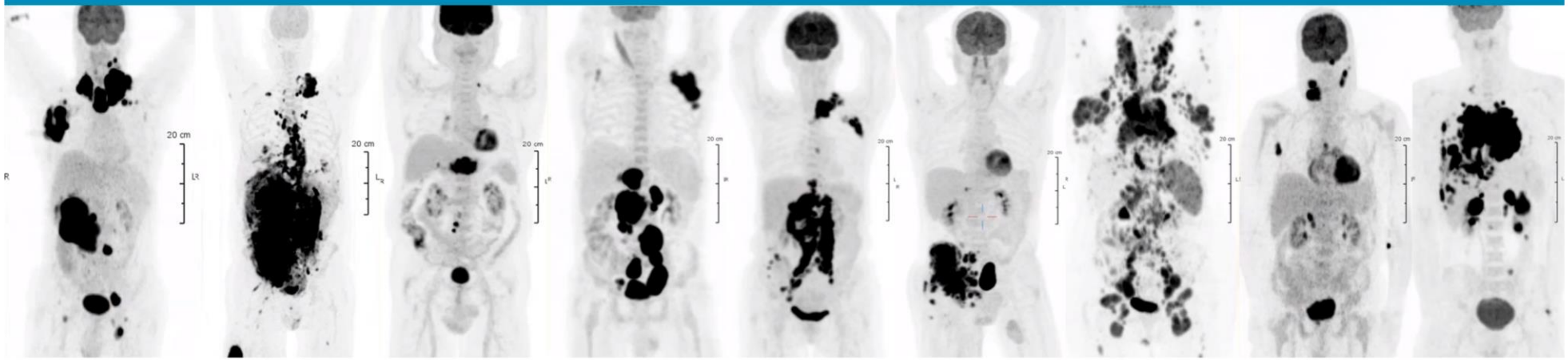

Background

- Recent interest in FDG PET/CT radiomics with machine learning for prognosis and treatment response prediction in DLBCL
- ML requires large datasets for training, cross-validation and external testing
- PET datasets are usually small (n<500)

Aim

- There is a general understanding that external testing is needed, but reviewers often ask for hold-out testing. Does this make sense?

- Using a clinical trial simulation to validate the performance of ML models by:
  - cross-validation (CV) **versus**
  - holdout and/or external testing

CV, holdout and external dataset

- Cross-validation:
  - train on x% and validate on (100-x)%
  - 5 fold CV is 80% train, 20% validate – choose different fold
  - Repeat with random reshuffling of data
- Hold-out: generate 'external' dataset by upfront keeping subsample separate. Use rest for CV training, and test on hold-out.
  - Pro: allows testing of model with data not used for training
  - Con: data (quality, demographics) is 'identical' – does not prove generalizability
- External dataset: data collected elsewhere, different scanner etc
  - Pro: data is really independent and different
  - Con: is one external dataset really enough? What does it prove?

Setup of simulation study (1)

- Input data (n=296) derived from actual DLBCL FDG PET/CT studies and clinical information (HOVON84):

Stage	Number of patients (%)	Log-SUVpeak	Log-Volume	Log-DMaxBulk	Prevalence of IPage=1 (%)	Prevalence of WHO=1 (%)
2	16	2.78 ±0.50	12.0±1.5	4.74±0.6	30	23
3	21	2.78 ±0.50	12.0±1.5	5.4±0.6	30	16
4	63	2.84 ±0.50	13.0±1.5	5.8±0.6	30	6

Model to predict probability

- Log(p) =

  -6.53+(0.533*LogVol)+(1.40*LogPeak)+(0.0027*DmaxBulk)+(0.77*IPIage)+(0.78*WHO1)

- p>0.4 predicts outome = 1

To match with incorrect prediction prevelance as seen in clinical data:

- Predicted outcome=1, 50% randomnly reset to 0
- Predicted outcome =0, 13% randomnly reset to 1
- This results in ROC-AUC = 0.72

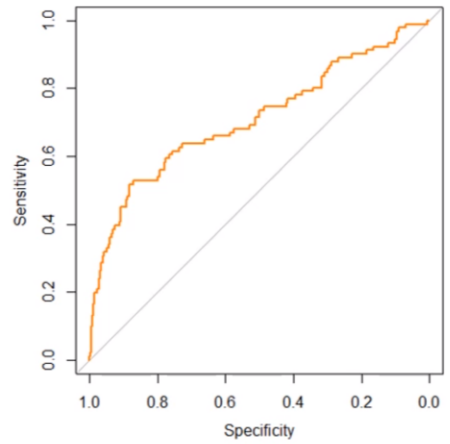

Simulations

N=500 cases, same prevalence of stage 2,3 and 4 as clinical data

1. 100 repeats of 5-fold stratified cross-validation (training=400, validation=100)

2. Hold-out (external) test, stratified, n=100
   Training and validation, 5-fold cross-validation, n=400
   - Steps repeated 100x

3. Training and validation, 5-fold cross-validation, n=500
   Newly simulated external dataset
   1. Same settings as training dataset
   2. Repeated 100x

4. ML Methods: LR, LDA, SVM and RF

5. Performance: ROC-AUC

Summary of findings

Theoretical AUC =0.72

Simulation 1, n=500, 5 fold repeated stratified cross-validation
CV area under the ROC curves were:
LR = 0.70±0.06
LDA = 0.70±0.05
SVM = 0.69±0.05
RF = 0.68±0.05

Simulation	LR AUC-CV
1. Reference - 5-fold cross-validation (each fold n=100)	0.70 ± 0.06
2. Hold-out test set (n=100)	0.70 ± 0.07
3A. New external dataset - representative for training set (n=100)	0.70 ± 0.06

Sim 3: external dataset – 100 replicates

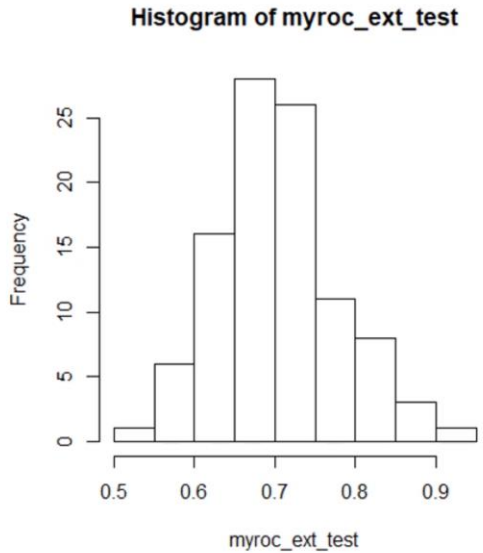

- N=500 for CV training
- External dataset (n=100) was regenerated 100x
- Data and patient characteristics equal to training dataset
- For each replication we calculated the AUC

- Histogram shows variability in AUC across external datasets (mean and SD are the same as seen with cross-validation in training dataset)

- A single point estimate of AUC may vary between 0.5 up to 0.9 -> this means that a single external dataset may show performance anywhere between 0.5 and 0.9

External dataset sample size– 100 replicates

N=100

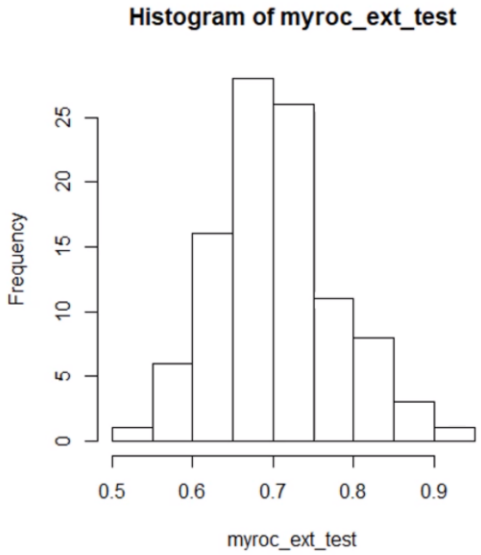

n=200

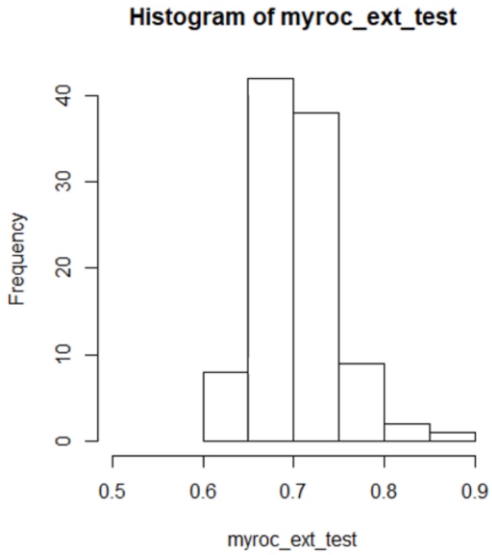

n=500

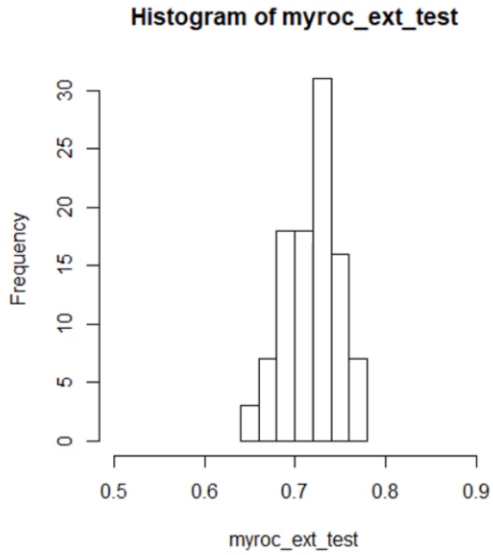

Sample size of external dataset determines (obviously) precision of external test AUC

Main findings

- Hold-out (internal) test dataset no added value compared with cross-validation
- External test dataset that is very comparable (same methods, same patient characteristics) has statistically no added value to cross-validation.
  - Often only 1 external dataset is available – a single point AUC estimate may not be representative depending on sample size (needs to be large)
- External test dataset, dissimilar regarding methodology, may prove generalizability of model:
  - need to adapt thresholds
  - OR to transform input data (retrospectively with COMBAT)
  - OR use standards to avoid methodological variability
- External test dataset dissimilar regarding patient stage prevalence (data not shown)
  - Results can be more optimistic or pessimistic simply because different prevalence of outcome – may NOT prove or discard model performance (data not fully shown)
  - Mainly illustrates (lack of) generalizability to different patient populations

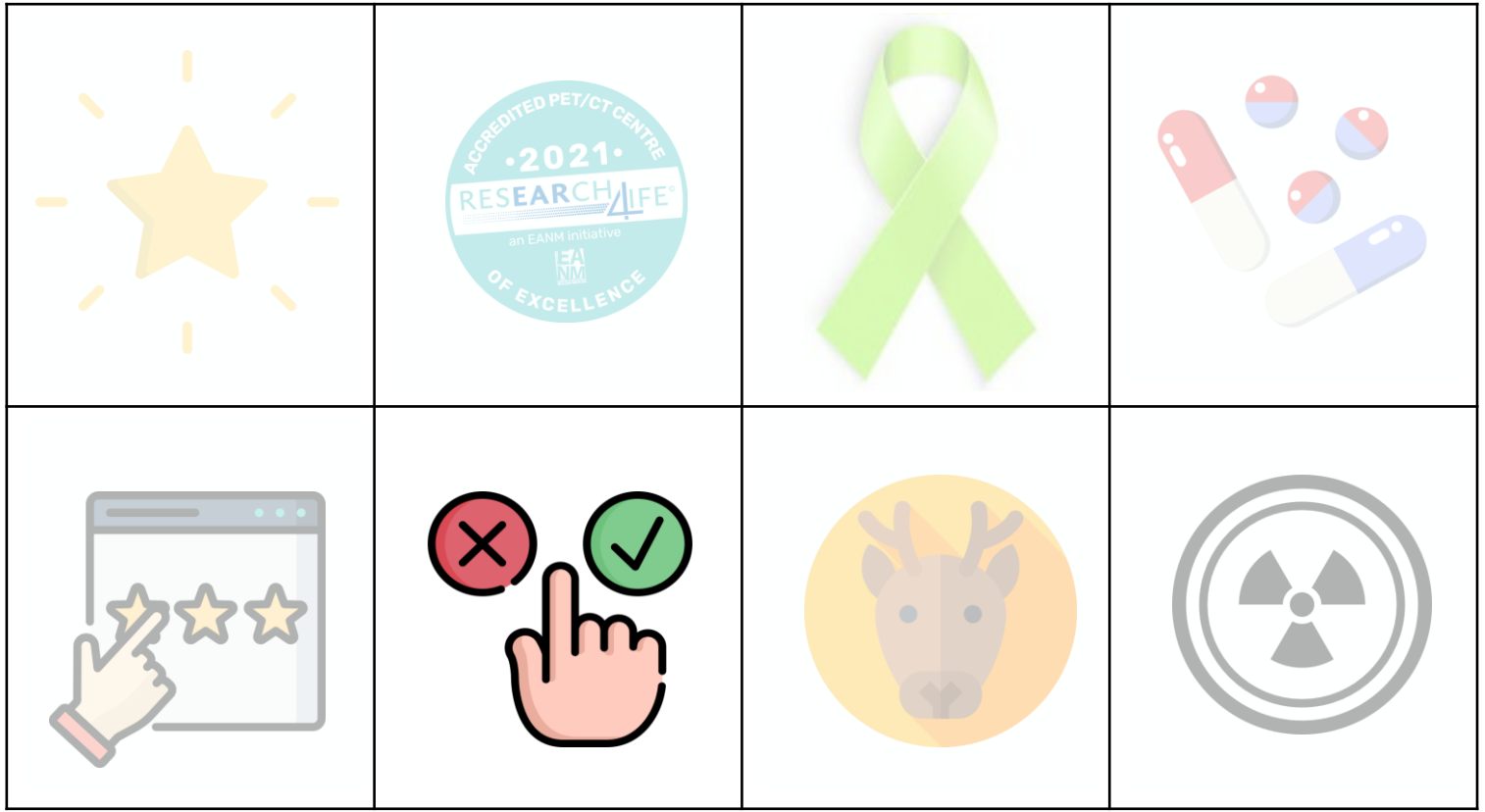
ACCREDITED PET/CT CENTRE
·2021·
RESEARCH4LIFE
an EANM initiative
OF EXCELLENCE

Postsurgical Gleason score prediction enhanced by PSMA PET/MRI radiomics

Esteban Lucas **SOLARI,** Andrei **GAFITA;** Sylvia **SCHACHOFF;** Borjana **BOGDANOVIĆ;** Alberto **VILLAGRÁN ASIARES;** Isabel **RAUSCHER;** Dimitris **VISVIKIS;** Wolfgang **WEBER;** Nassir **NAVAB;** Matthias **EIBER;** Mathieu **HATT;** Stephan G. **NEKOLLA**

EANM'21 WORLD LEADING MEETING VIRTUAL

20-23 Oct 2021

Contact: *elucas.solari@tum.de*

This project has received funding from the European Union's Horizon 2020 research and innovation programme under the Marie Sklodowska-Curie grant agreement No 764458.

Why radiomics to predict Gleason score?

Gleason score

ISUP

Gleason score	ISUP grade
2-6	1
7 (3+4)	2
7 (4+3)	3
8 (4+4 or 3+5 or 5+3)	4
9-10	5

Prostatectomy vs Biopsy

"The meta-analysis found that prostatectomy Gleason grade was accurately predicted in 63%, upgraded in 30%, and downgraded in 7% of patients."

* Cohen MS, Hanley RS, Kurteva T, Ruthazer R, Silverman ML, Sorcini A, Hamawy K, Roth RA, Tuerk I, Libertino JA, "*Comparing the Gleason prostate biopsy and Gleason prostatectomy grading system: the Lahey Clinic Medical Center experience and an international meta-analysis*" (2008)

© HYBRID – H2020-MSCA-ITN-2017 Marie Skłodowska-Curie Grant Agreement No 764458 HYBRID

Previously...

Cohort (N>130)

68Ga-PSMA PET/MRI

Radiomics

IBSI
image biomarker standardisation initiative

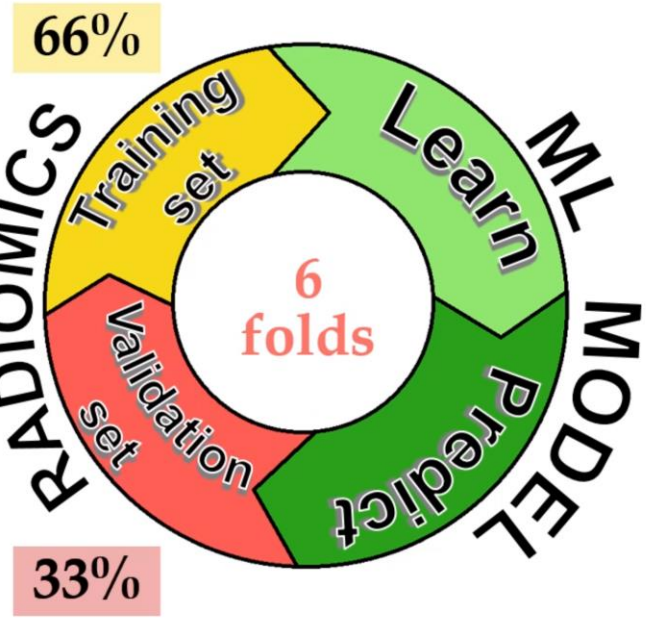

* **Solari EL**, Gafita A, Schachoff S, Bogdanović B, Villagrán Asiares A, Amiel T, Hui W, Rauscher I, Visvikis D, Maurer T, Schwamborn K, Mustafa M, Weber W, Navab N, Eiber M, Hatt M, Nekolla SG, "*The added value of PSMA PET/MR radiomics for prostate cancer staging*" (2021)

© HYBRID – H2020-MSCA-ITN-2017 Marie Skłodowska-Curie Grant Agreement No 764458 HYBRID

Previously...

PET+ADC

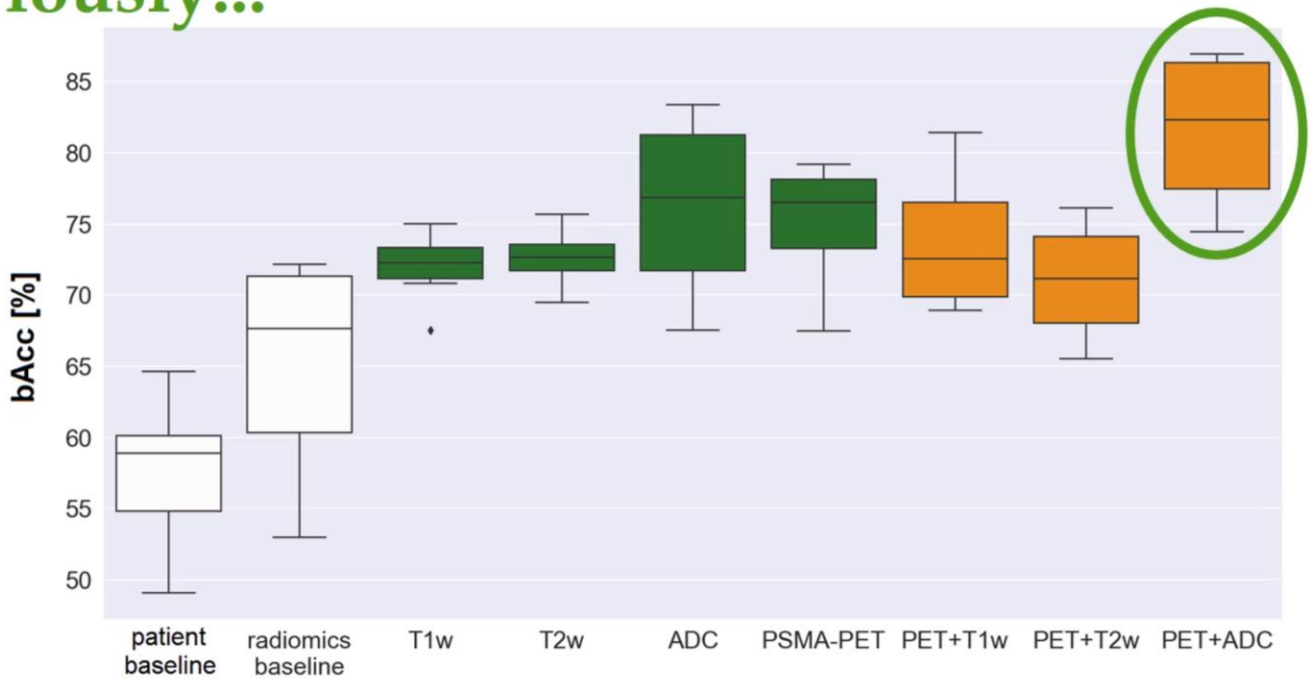

* **Solari EL**, Gafita A, Schachoff S, Bogdanović B, Villagrán Asiares A, Amiel T, Hui W, Rauscher I, Visvikis D, Maurer T, Schwamborn K, Mustafa M, Weber W, Navab N, Eiber M, Hatt M, Nekolla SG, "*The added value of PSMA PET/MR radiomics for prostate cancer staging*" (2021)

© HYBRID – H2020-MSCA-ITN-2017 Marie Skłodowska-Curie Grant Agreement No 764458 HYBRID

Objectives of this work

Test PET+ADC radiomics model in the prediction of postsurgical Gleason score (psGS).

Compare it to biopsy Gleason score (bGS).

© HYBRID – H2020-MSCA-ITN-2017 Marie Skłodowska-Curie Grant Agreement No 764458 HYBRID

Patient cohort

101 patients with both biopsy and postsurgical GS

	postsurgical Gleason score	biopsy Gleason score
ISUP 1-3:	60 (59%)	45 (45%)
ISUP 4:	23 (23%)	27 (27%)
ISUP 5:	18 (18%)	29 (29%)

© HYBRID – H2020-MSCA-ITN-2017 Marie Skłodowska-Curie Grant Agreement No 764458 HYBRID

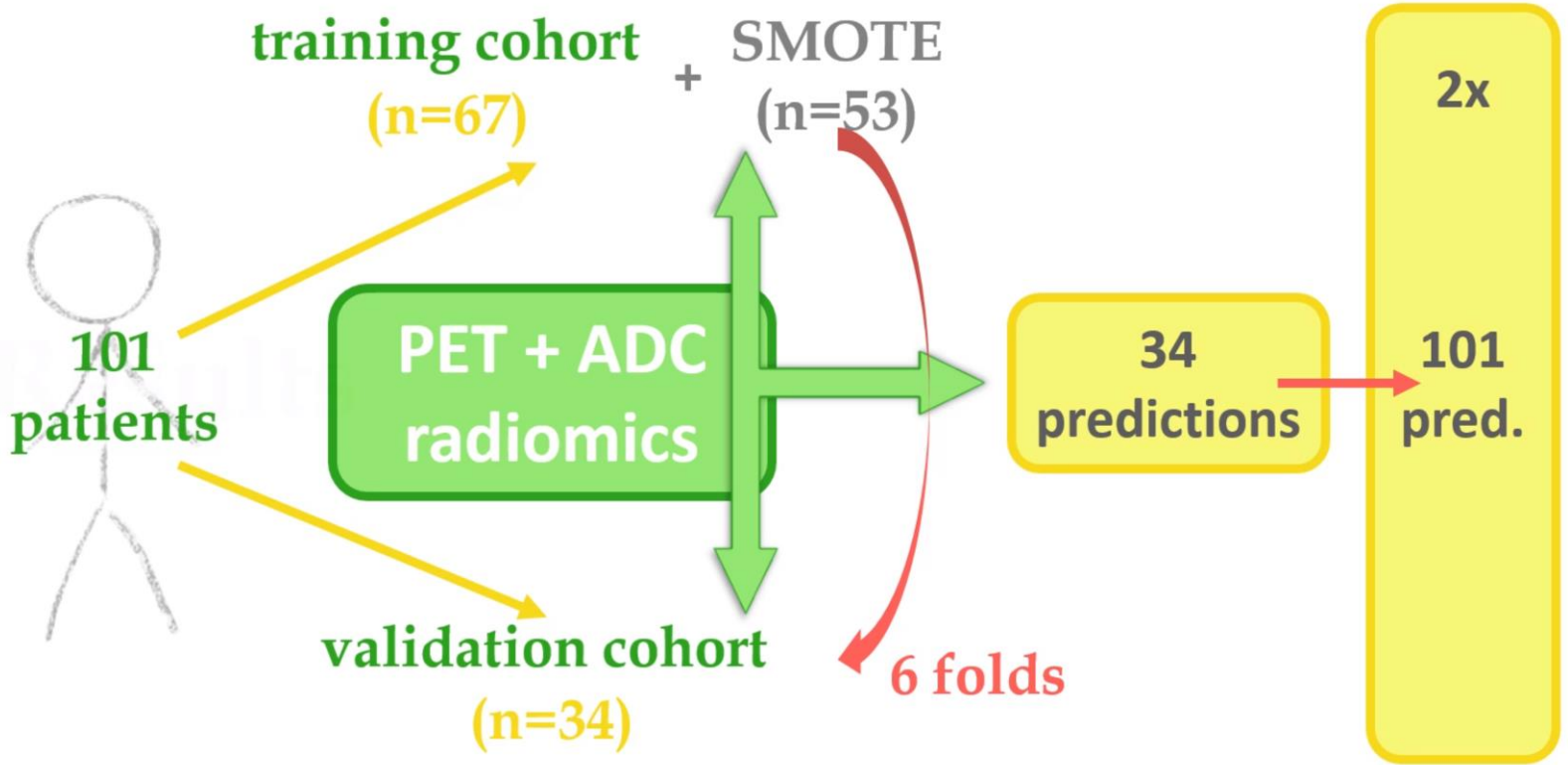

© HYBRID – H2020-MSCA-ITN-2017 Marie Skłodowska-Curie Grant Agreement No 764458 HYBRID

Accuracy

$$bAcc = \frac{1}{3}\left(\frac{TP_{GS<8}}{(TP+FN)_{GS<8}} + \frac{TP_{GS=8}}{(TP+FN)_{GS=8}} + \frac{TP_{GS>8}}{(TP+FN)_{GS>8}} \right)$$

Accuracy		
	Accuracy [%]	Balanced accuracy [%]
biopsy GS	70.4	72.4
radiomics	77.9	82.6

	bGS [%]	radiomics [%]
Upgraded	25.4	18.3
Predicted	70.4	77.9
Downgraded	4.2	3.8

Marie Skłodowska-Curie Grant Agreement No 764458 HYBRID

Conclusions

Our PET+ADC radiomics model outperformed biopsy Gleason score as a predictor of postsurgical Gleason score overall and in every GS group.

This hints at a clinical value of image-based models as an alternative to biopsy-based GS.

© HYBRID – H2020-MSCA-ITN-2017 Marie Skłodowska-Curie Grant Agreement No 764458 HYBRID


ACCREDITED PET/CT CENTRE
•2021•
RESEARCH4LIFE
an EANM initiative
OF EXCELLENCE

Sparse deep-learning: Multi-organ objective segmentation (MOOSE) for 18F-FDG PET/CT total body datasets

Lalith Kumar Shiyam Sundar[1], Josef Yu[1], Oana Kulturer[1], Barbara Fueger[1], Daria Kifjak[1], Thomas Nakuz[1], Hyung Min Shin[1], Annika Katherina Sima[1], Daniela Kitzmantl[1], Ramsey D Badawi[2], Simon R Cherry[2], Benjamin A Spencer[2], Marcus Hacker[1], Thomas Beyer[1]

[1] Medical University of Vienna, Vienna, Austria
[2] University of California Davis, California, United States

Objective

To build a clinical total-body PET/CT atlas for probing inter-organ communication using total-body PET/CT

Long axial field-of-view PET/CT

PET/CT image

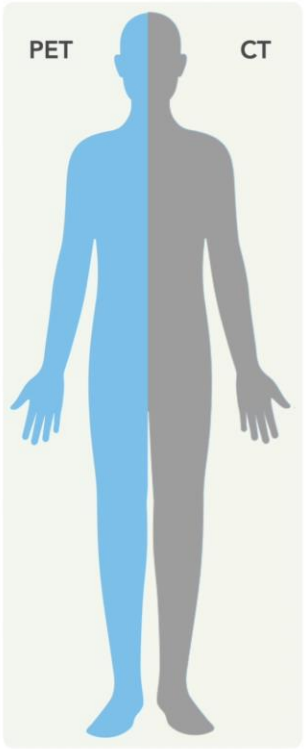

Total-body PET/CT atlas

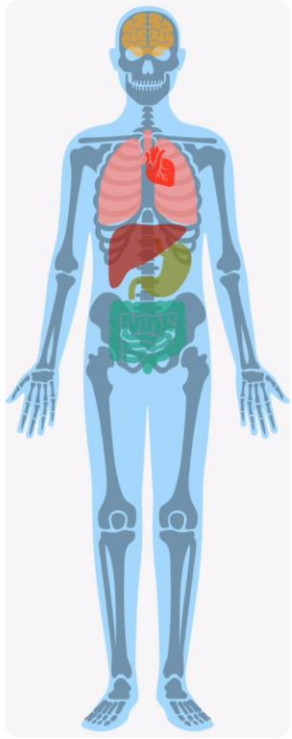

Total-body PET spatio-temporal network analysis

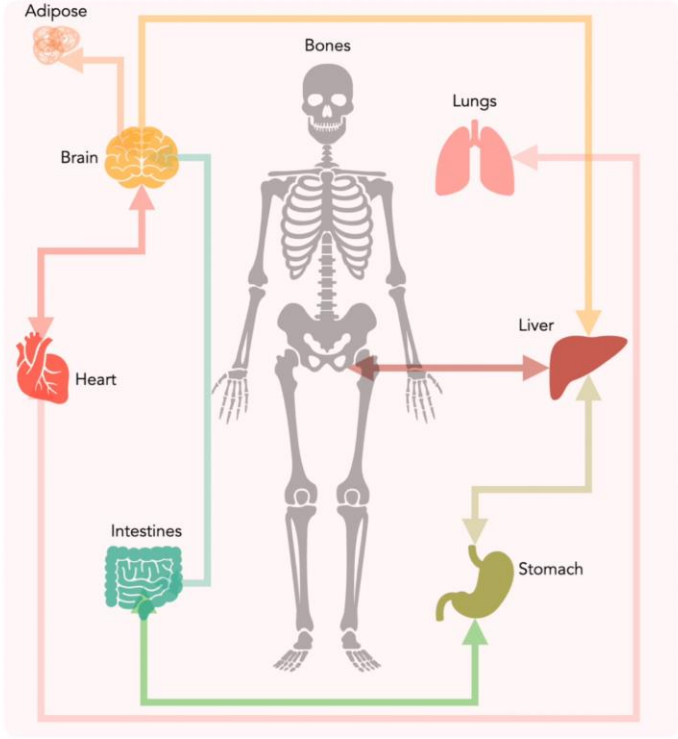

Challenges

Subject variability

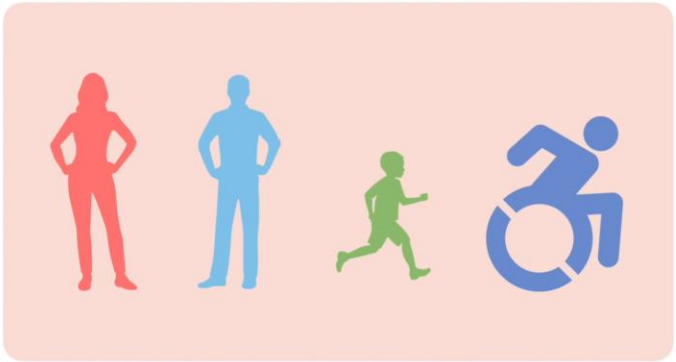

Scanner variability

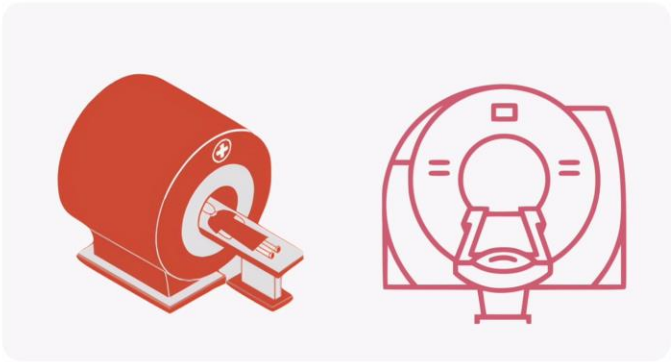

3D semantic segmentation

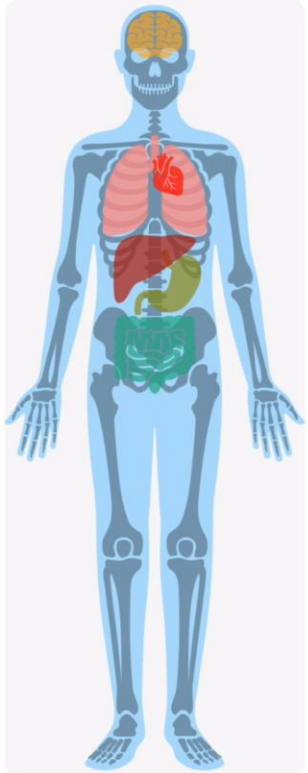

Morphological variability

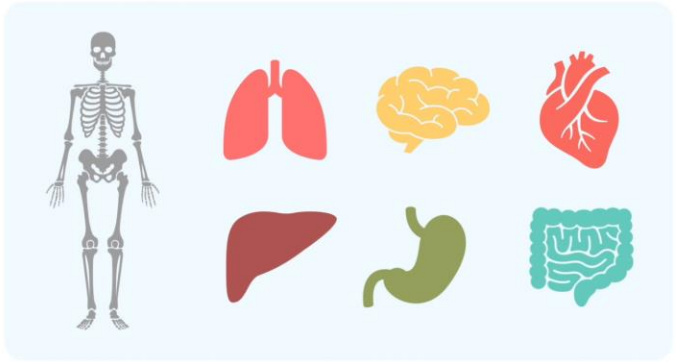

Sparse datasets

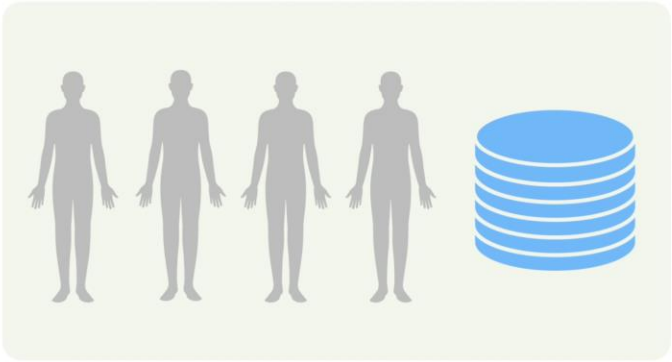

MEDICAL UNIVERSITY OF VIENNA

Total-body medical semantic segmentation is complex

Proposed solution

Subject variability

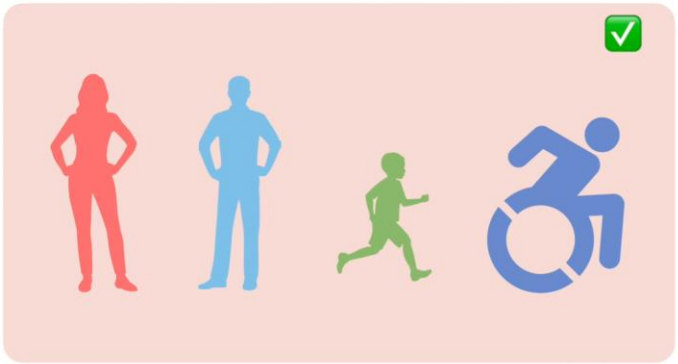

Scanner variability

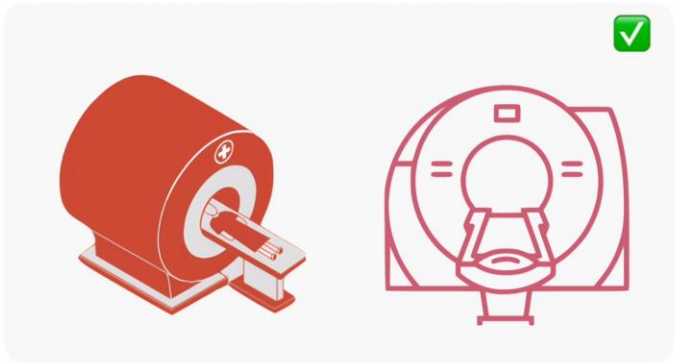

3D semantic segmentation

3D U-Net based Deep-learning

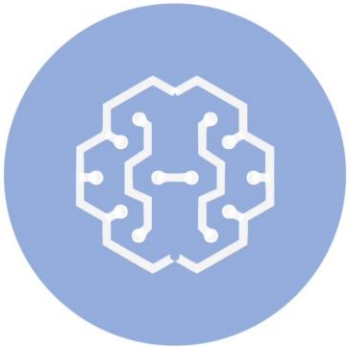

Morphological variability

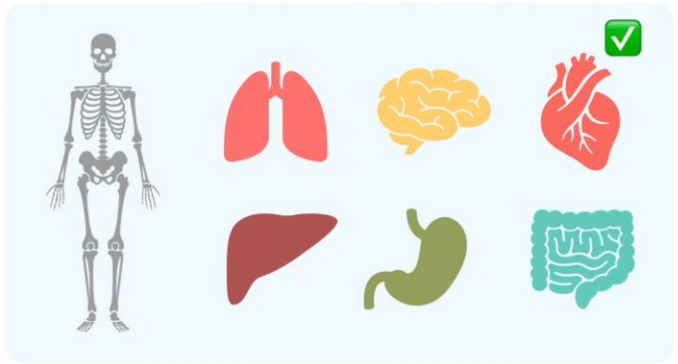

Sparse datasets

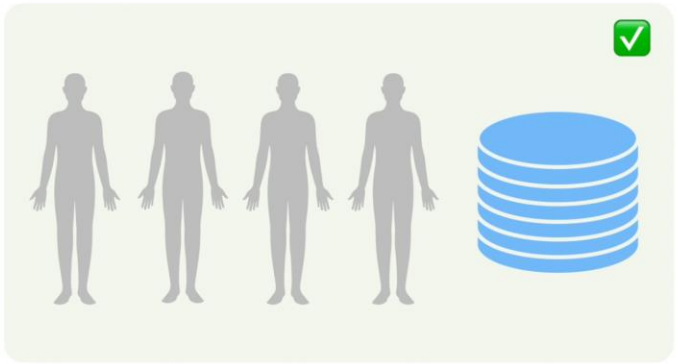

MEDICAL UNIVERSITY OF VIENNA

3D U-Net based Deep-learning: A promising solution for semantic segmentation

Methodology

MOOSE: Multi-Organ Objective SEgmentation

MOOSE
Multi-Organ Objective SEgmentation
Powered by QIMP

2 x Nuc.Med
2 x Rad

4 x Med students

51 LD-CT, PET and MR
uEXPLORER
+
Siemens datasets

Organs

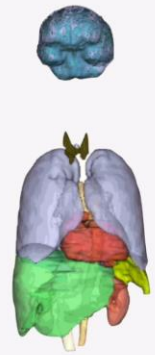

2 x Nuc.Med
2 x Rad

Bones

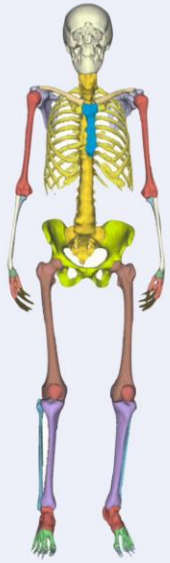

4 x Med students

Fat, muscle and 83 Brain regions

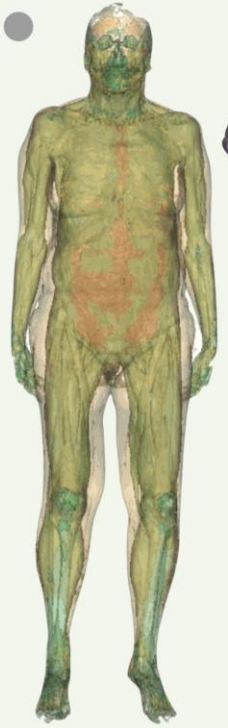

Reference standard for brain regions derived using integrated PET/MR data and Hammersmith atlas

MEDICAL UNIVERSITY OF VIENNA

MOOSE reference segmentations comprises of 120 tissue classes

Inter-variability issues

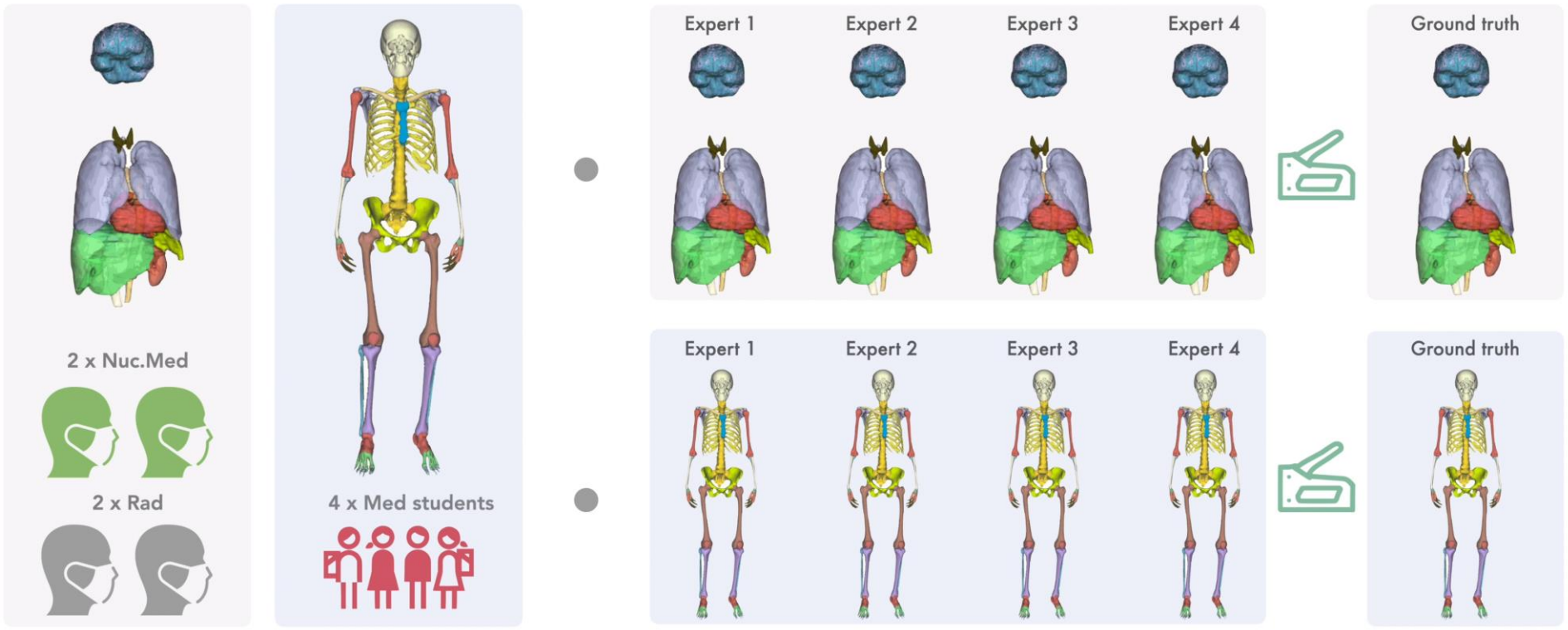

Methodology

Muscle and fat: Semi-automated thresholding

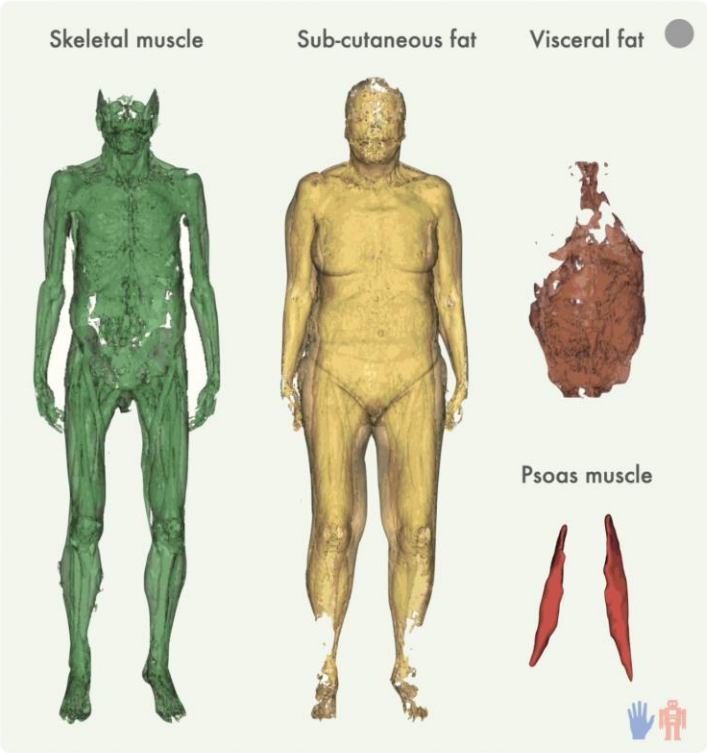

Atlas based 83 brain sub-region segmentation

Goal: Segment PET brain into 83 sub-regions of Hammersmith atlas

[1] Utilise simultaneous PET/MR brain data and normalise coregistered MR data to Atlas space

[2] Use the inverse transform to bring the atlas to native space and propagate it to PET

3D U-Net deep learning

Organs

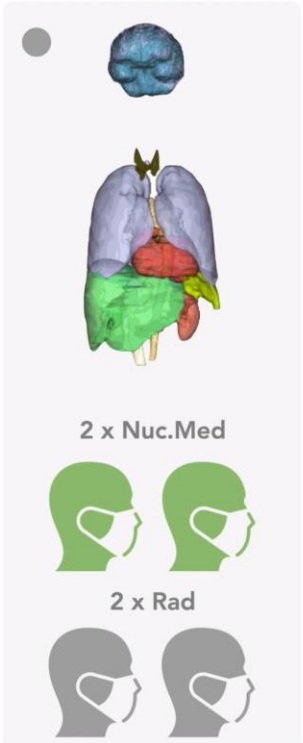

Bones

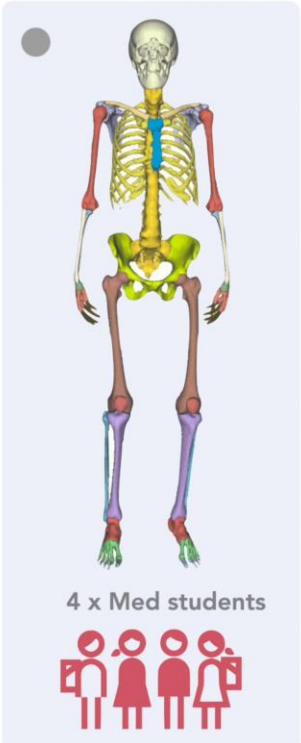

Fat, muscle and 83 Brain regions

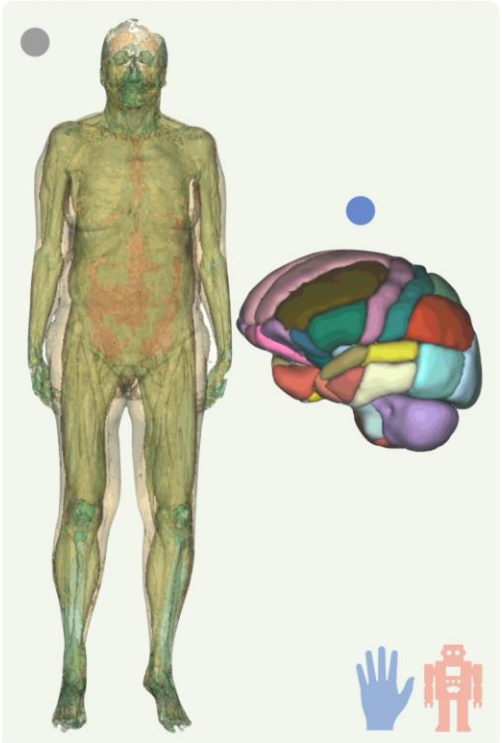

40 Training / 11 test datasets

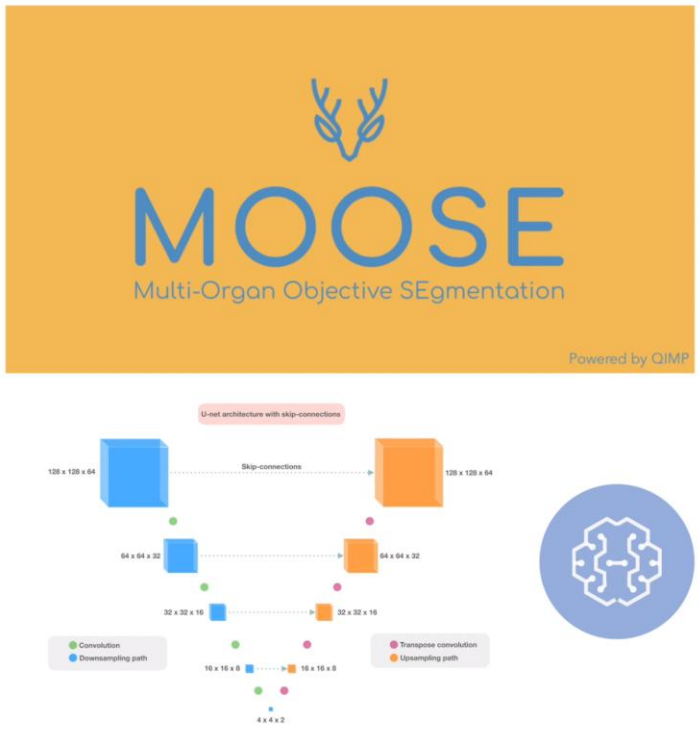

Results

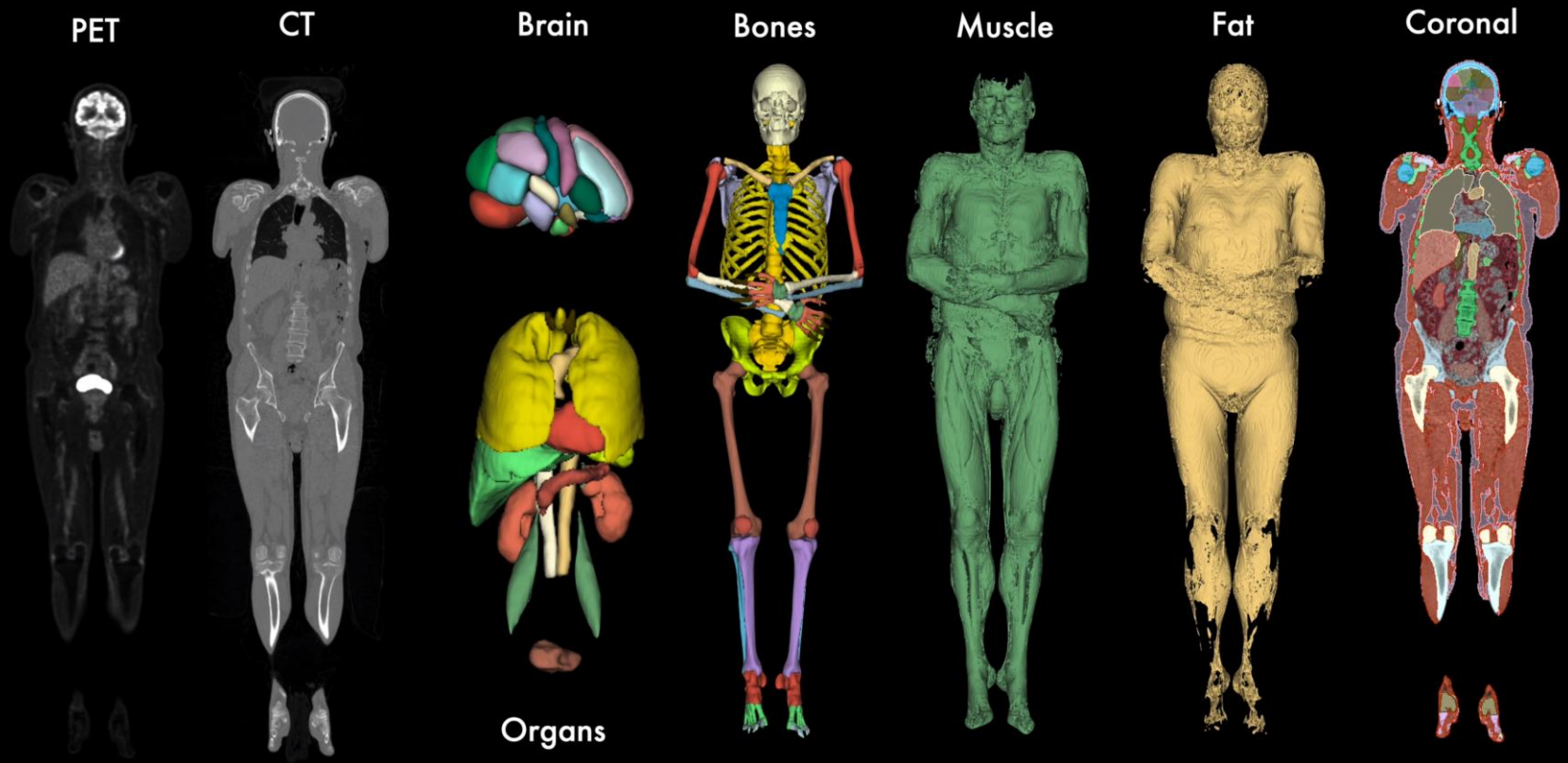

MEDICAL UNIVERSITY OF VIENNA

MOOSE[120] is able to achieve 3D semantic segmentation

Results: Dice coefficients

Organs (>0.90)

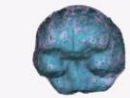

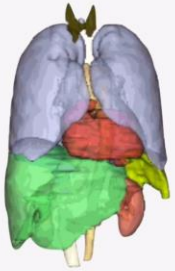

Adrenal glands: 0.92
Aorta: 0.98
Bladder: 0.91
Whole Brain: 0.99
Heart: 0.97
Kidneys: 0.97
Liver: 0.99
Pancreas: 0.91
Spleen: 0.98
Thyroid: 0.98
Vena cava: 0.95
Lung: 0.99

Brain (>0.70)

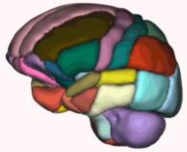

83 Hammersmith regions

Bones (>0.80)

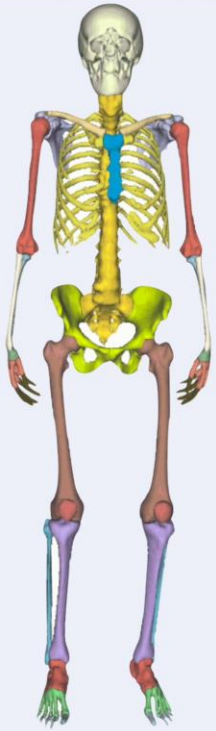

Carpal: 0.83
Clavicle: 0.94
Femur: 0.98
Fibula: 0.95
Fingers: 0.89
Humerus: 0.97
Metacarpal: 0.86
Metatarsal: 0.92
Patella: 0.97
Pelvis: 0.95
Radius: 0.92
Ribcage: 0.89
Scapula: 0.95
Skull: 0.96
Spine: 0.94
Sternum: 0.89
Tarsal: 0.97
Tibia: 0.97
Toes: 0.86
Ulna: 0.94

Muscle and fat (>0.90)

Skeletal muscle: 0.96

Sub-cutaneous fat: 0.96

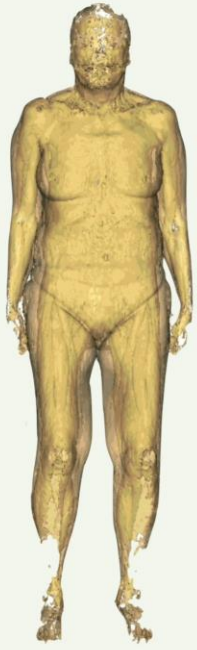

Visceral fat: 0.94

Psoas muscle: 0.90

MEDICAL UNIVERSITY OF VIENNA

MOOSE[120] segmentations from CT produce better DICE scores than PET

Out-of-distribution study

How does MOOSE handle out-of-distribution datasets?

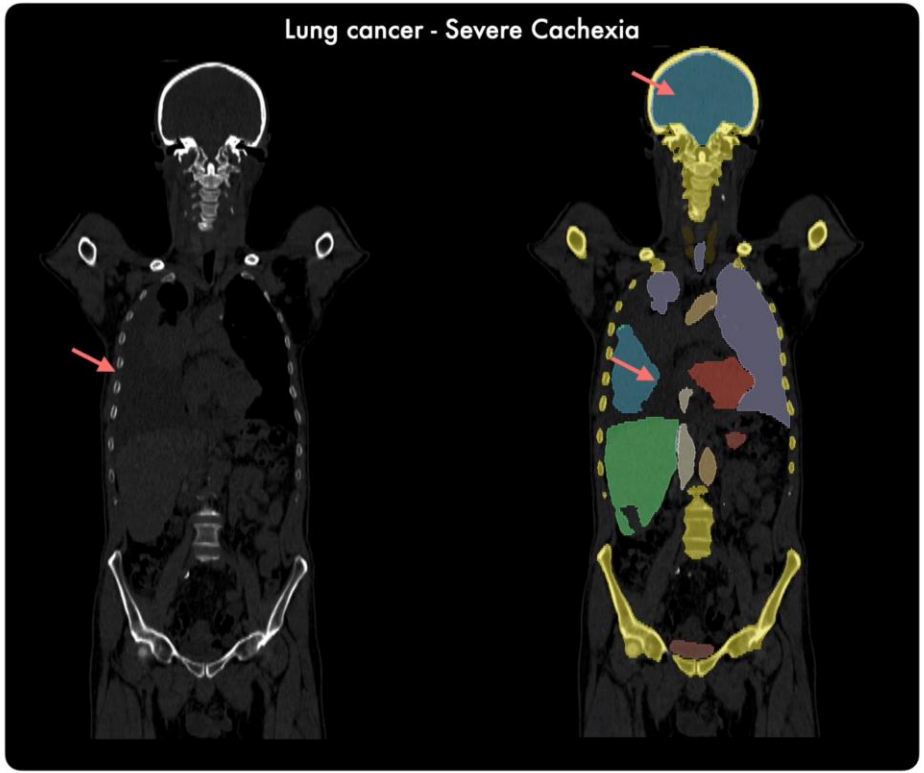

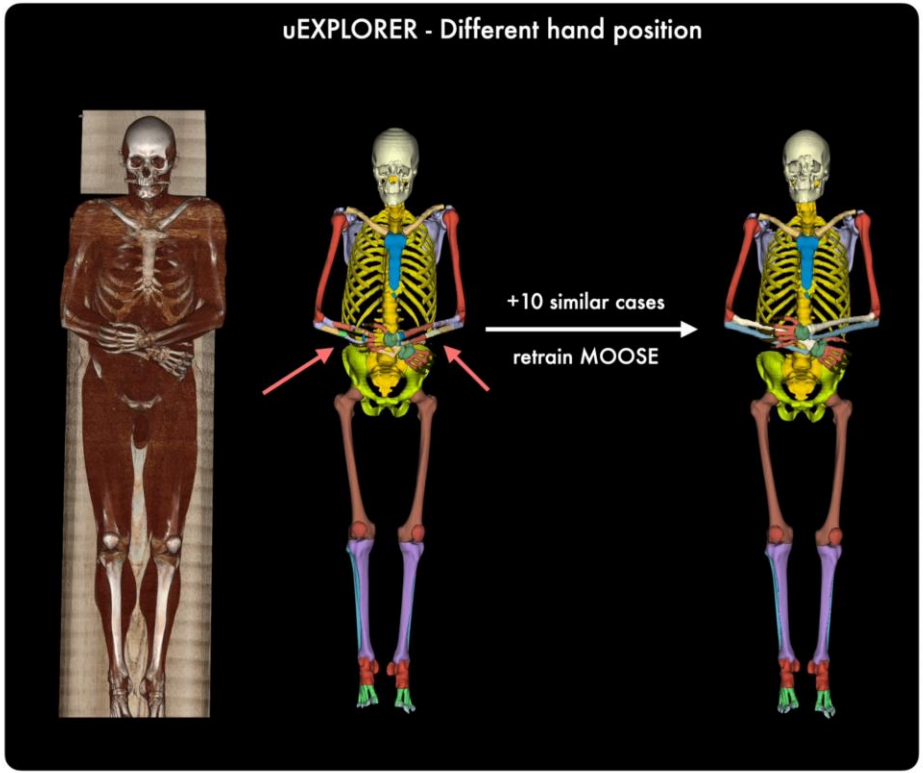

*Data provided by Armin Frille, Swen Hesse, Osama Sabri (University Hospital Leipzig)

Summary

An open-source total-body PET/CT atlas (manuscript in submission)

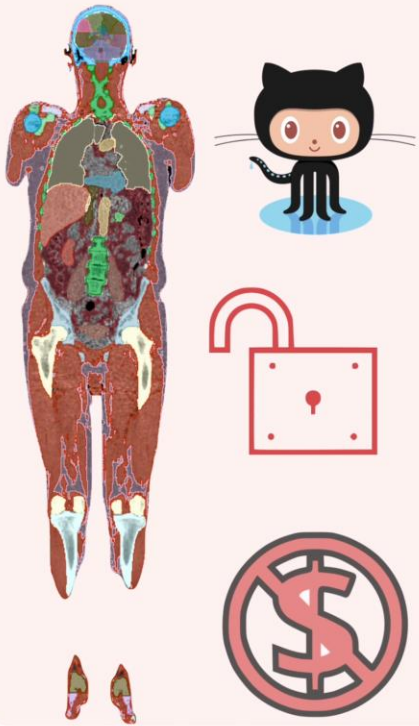

Works reasonably well with 'usual' scenarios

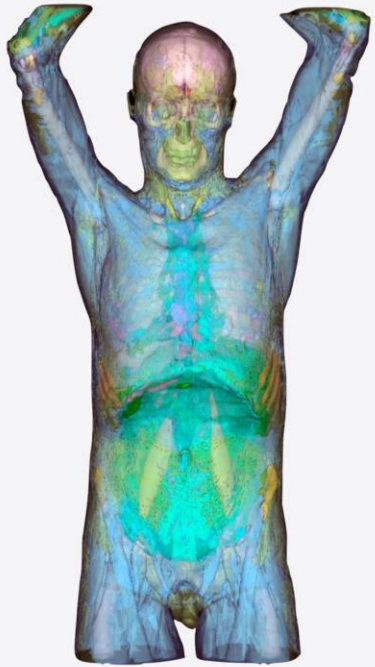

Datasets with increased variability (not size) can make MOOSE robust

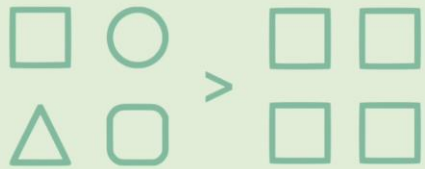

High-performance computing is key

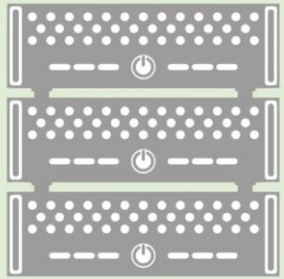

MEDICAL UNIVERSITY OF VIENNA

Sparse data with rich variability > Large dataset with minimum variability

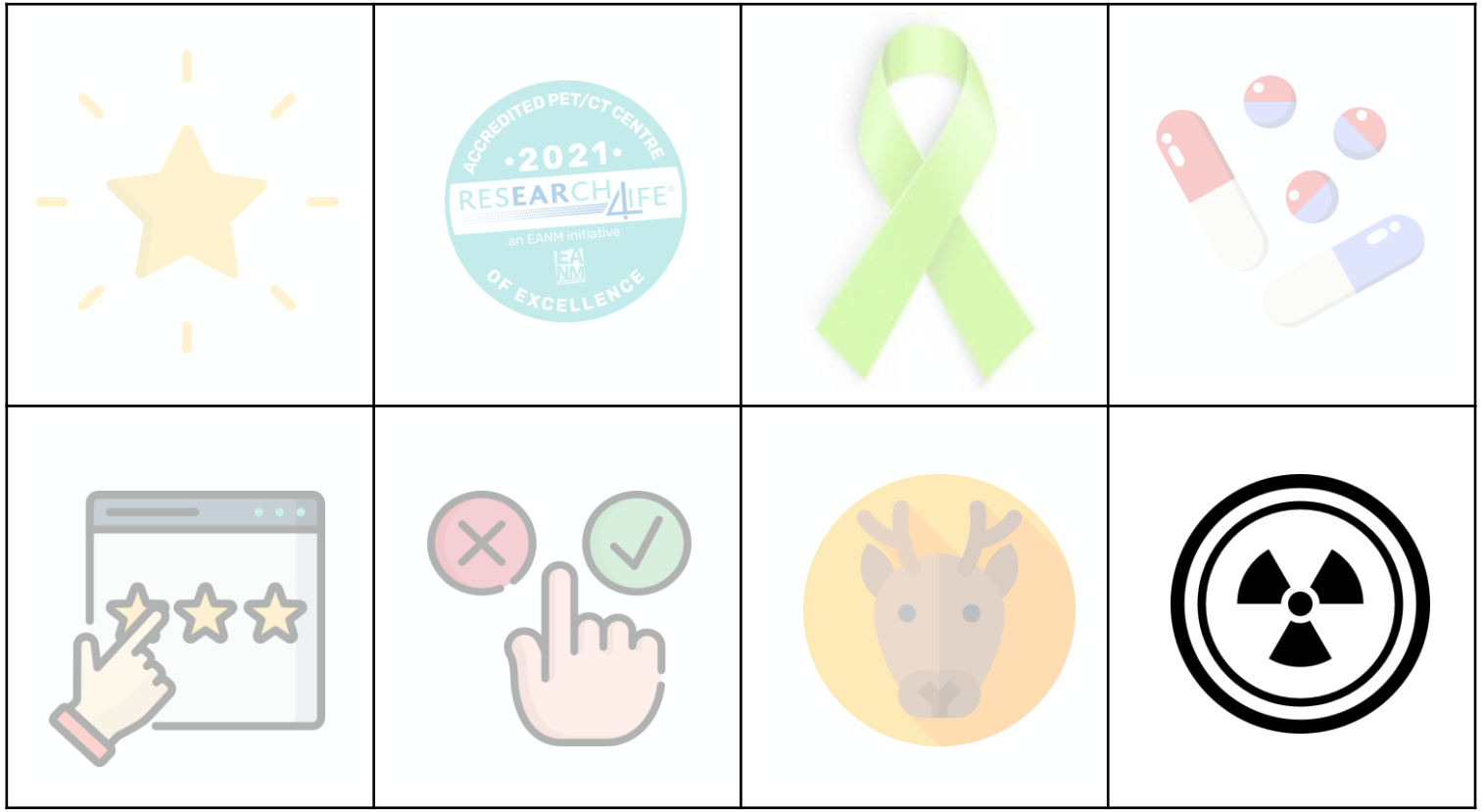
ACCREDITED PET/CT CENTRE
•2021•
RESEARCH4LIFE
an EANM initiative
OF EXCELLENCE

Title

Quantitative assessment of ^{123}I-MIBG uptake in children in determining the unfavorable histological type of neuroblastoma

Nr. EP-157

Keywords / Topics B91 Paediatric Study

Authors Mikhail Yadgarov [1] , Nikolai Matveev [2] , Kailash Chaurasiya [1] , Elena Kireeva [1] , Yury Likar [1]

[1] Dmitry Rogachev National Medical Research Center, Moscow, Russian Federation , [2] Russian National Research Medical Univercity, Moscow, Russian Federation

Aim

Neuroblastoma (NB) is the most common extracranial solid tumor in childhood. Scintigraphy with ^{123}I-MIBG combined with the SPECT / CT protocol is an integral part of the diagnostic examination for NB staging. In recent years, data have emerged on the possible relationship between the degree of ^{123}I-MIBG accumulation and the histological variant of NB [1-2].
Currently, it is possible to use the semi-quantitative parameter SUVmax (maximum standardized uptake value) obtained from SPECT with ^{123}I-MIBG, and this parameter has found wide application in positron emission tomography (PET).
The only way to reliably determine the histological type of tumor is a biopsy followed by staging according to the criteria of the INPC international classification. However, biopsy is performed under anesthesia and is an invasive procedure that can be accompanied by the development of undesirable consequences, and it takes a certain amount of time to obtain the results of a histological examination. In addition, obtaining biopsies from all tumor sites is impossible, and since NB is a spatially heterogeneous tumor, the risk of uninformative examination increases.
The method of non-invasive determination of the histological variant together with additional clinical and imaging data (CT, MRI) in neurogenic tumors in children may be of great clinical importance for the choice of patient management tactics (biopsy, extended surgery, polychemotherapy). Therefore, the development of algorithms for non-invasive differential diagnosis of the histological type of neuroblastoma based on the analysis of parameters for quantitative assessment of the accumulation of ^{123}I-MIBG in SPECT / CT may have a certain clinical significance.The aim of our work was to determine the significance of the quantitative assessment of SUVmax in the non-invasive determination of an unfavorable histological type of neuroblastoma, which is associated with a poor prognosis.

Materials and Methods

Patients.

The retrospective analysis included 153 pre-therapy patients with neuroblastoma; the median age was 17.7 months (range 1 to 125). 122 patients (79.7%) had a poorly differentiated (unfavorable) variant of neuroblastoma and 31 patients (20.3%) had a highly differentiated variant (ganglioneuroma). All patients underwent ^{123}I-MIBG scintigraphy with an additional SPECT / CT protocol of the region of interest on a two-detector gamma camera (Discovery 670, GE Healthcare, USA) after 24 hours of a radiopharmaceutical administration.

Image analysis.

The accumulation of the ^{123}I-MIBG in the primary tumor was assessed using the work station with the calculation of the SUVmax parameter. To assess the SUVmax, a two-detector gamma camera was calibrated using a phantom containing an isotope and a CT phantom. Then, the obtained values were integrated into the HERMES Medical Imaging suite software (Hermes Medical Solutions, Stockholm, Sweden), and immediately before the analysis, the administered ^{123}I-MIBG activity and the time of administration for each patient were entered into the protocol of the HERMES Medical Imaging software and the obtained images were reconstructed. On the reconstructed images, the maximum accumulation in tumor tissue was assessed using an SUV using the HERMES Medical Imaging suite software (Figure 1).

Statistical analysis.

Intergroup analysis was performed using the Mann Whitney U-test, the optimal cut-off value for the SUVmax parameter was selected based on the optimal sensitivity / specificity ratio according to the results of the ROC analysis. Additionally, Kaplan-Meier curves with respective log- rank tests were calculated following binarization of metric parameter using cut-off values defined by receiver operating characteristic. Fisher's exact test was used to compare binary variables. Statistical analysis was performed using the IBM SPSS Statistics for Windows, Version 25 (IBM SPSS Statistics for Windows, IBM Corporation, Armonk, NY)

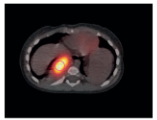

Fig. 1: Figure 1. Quantitative assessment of MIBG uptake (SUVmax) in NB patient on SPECT/CT images

Results

Patients with an unfavorable histological variant of neuroblastoma had significantly higher SUVmax values in comparison with patients with a favorable variant: median 5.5 [3.3; 8.3] versus 2.9 [1.6; 4.4], p<0.001. In the presence of a poorly differentiated variant of NB (unfavorable histological variant), patients were significantly more likely to have retroperitoneal and bilateral tumor localization (p = 0.001), the presence of metastatic lesions was noted with a greater frequency (p <0.001), 4 stage according to the INSS system, M stage according to INRGSS were more often recorded, and with amplification of the MYCN oncogene and deletion of 1p, the chance of having an unfavorable histological variant increased by 35.82 (95% CI: 4.96-258.52) and 7.66 (95% CI: 2.39-24.58) times, respectively.

The differences in event-free and overall survival in patients with favorable / unfavorable histological variants are statistically significant: three-year event-free and overall survival in patients with favorable histological variants were 91.1 ± 3.2% and 96.5 ± 2.5%, respectively; in patients with an unfavorable histological variant - 61.1 ± 2.1% and 81.5 ± 1.7%, respectively (Fig. 2, log-rank test, p <0.001; Fig. 3, log-rank test, p <0.001).

The AUC for SUVmax was 0.769 (95% CI: 0.642; 0.895), the optimal cut-off value was 3.74, allowing oncologists to classify patients according to the degree of tumor differentiation with 71.0% sensitivity and 70.6% specificity (Fig. 4).

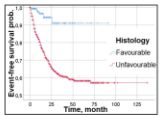

Fig. 2: Kaplan-Meier curves - overall survival in patients with favorable and unfavorable histological variants of neuroblastoma

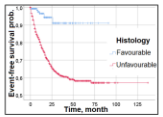

Fig. 3: Kaplan-Meier curves - event-free survival in patients with favorable and unfavorable histological variants of neuroblastoma

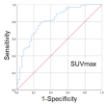

Fig. 4: ROC-curve - SUVmax parameter as a predictor of an unfavorable histological variant of NB

Conclusion

Method of non-invasive determination of histological type of neuroblastoma, based on an SUVmax assessment, together with the additional data may have important implications for clinical management of patients with neuroblastoma.

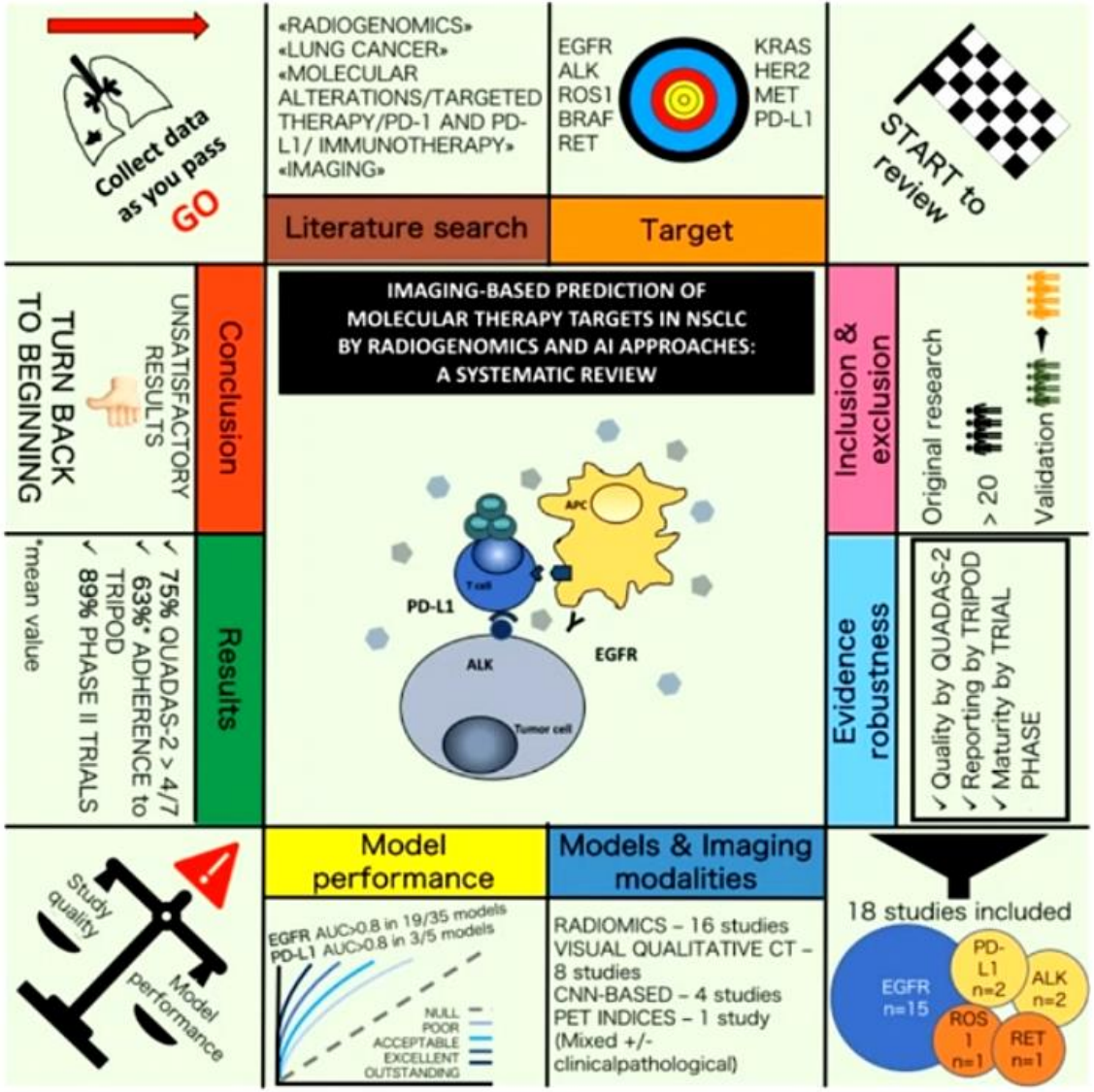
Collect data as you pass GO
«RADIOGENOMICS»
«LUNG CANCER»
«MOLECULAR ALTERATIONS/TARGETED THERAPY/PD-1 AND PD-L1/ IMMUNOTHERAPY»
«IMAGING»
Literature search
EGFR
ALK
ROS1
BRAF
RET
KRAS
HER2
MET
PD-L1
Target
START to review
IMAGING-BASED PREDICTION OF MOLECULAR THERAPY TARGETS IN NSCLC BY RADIOGENOMICS AND AI APPROACHES: A SYSTEMATIC REVIEW
TURN BACK TO BEGINNING
UNSATISFACTORY RESULTS
Conclusion
Inclusion & exclusion
Original research
> 20
Validation
*mean value
✓ 75% QUADAS-2 > 4/7
✓ 63%* ADHERENCE to TRIPOD
✓ 89% PHASE II TRIALS
Results
Evidence robustness
✓ Quality by QUADAS-2
✓ Reporting by TRIPOD
✓ Maturity by TRIAL PHASE
APC
T cell
PD-L1
EGFR
ALK
Tumor cell
Study quality
Model performance
Model performance
Models & Imaging modalities
EGFR AUC>0.8 in 19/35 models
PD-L1 AUC>0.8 in 3/5 models
NULL
POOR
ACCEPTABLE
EXCELLENT
OUTSTANDING
RADIOMICS – 16 studies
VISUAL QUALITATIVE CT – 8 studies
CNN-BASED – 4 studies
PET INDICES – 1 study
(Mixed +/- clinicalpathological)
18 studies included
EGFR n=15
PD-L1 n=2
ALK n=2
ROS 1 n=1
RET n=1

Dates & Deadlines

March 2022	Congress Website opens
March 2022	Start Abstract Submission
Spring 2022	Registration opens
April 25, 2022	Abstract Submission Deadline
June 21, 2022	Notification of Abstract Acceptance
June 30, 2022	Early Registration Deadline
September 2022	Lift of Abstract Embargo
October 5, 2022	Advanced Registration Deadline
October 15, 2022	Congress Opening
October 19, 2022	Congress Closing